Silica particle characterization

The size distributions of the silica particles were measured with a Zetasizer 3000HS (Worcestershire, United Kingdom) after sonication of the particles at a concentration of 300 μg/mL in H_2O.

Cytotoxicity assay and cytokine production assay

RAW264.7 cells (1.5×10^4 cells/well) were seeded in 96-well plates (Nunc, Rochester, NY), cultured at 37°C for 12 h, and then treated with each type of silica particle (100 μg/mL) or medium (for negative control) for 12 h. The cytotoxicity of the silica particles was assessed by means of the standard methylene blue assay method, as previously described (Morishige et al. 2010a). Production of tumor necrosis factor-α (TNFα) in culture supernatants was assessed by means of an enzyme-linked immunosorbent assay (ELISA) kit (BD Pharmingen, San Diego, CA) according to the manufacturer's instructions.

Inhibitory assay

RAW264.7 cells (1.5×10^4 cells/well) were seeded in 96-well plates (Nunc), cultured at 37°C for 12 h, and then preincubated for 2 h with SB203580 (50 μM), U0126 (50 μM), SP600125 (10 μM), BHA (50 or 250 μM), or DPI (2 or 10 μM). Then, the cells were treated with one type of silica particle (100 μg/mL) or medium (for negative control) for 4 h. TNFα production in the culture supernatants was assessed by means of an ELISA kit (BD Pharmingen) according to the manufacturer's instructions.

Western blotting analysis

RAW264.7 cells were seeded in 12-well plates, cultured at 37°C for 12 h, and then treated with one type of silica particle (100 μg/mL) or medium (for negative control) for 0.5, 1, 2, or 4 h. For positive control, cells were treated with lipopolysaccharide (LPS) (1.25 μg/mL) for 30 min. Cells were then washed with PBS and lysed with Mammalian Protein Extraction Reagent (M-PER; Thermo Fisher Scientific, Rockford, IL) containing a Halt Protease Inhibitor Cocktail Kit (Thermo Fisher Scientific) and Phosphatase Inhibitor Cocktail (Nacalai Tesque, Kyoto, Japan). Then protein samples (1–5 μg) were loaded on a 20% sodium dodecyl sulfate–polyacrylamide gel. After electrophoresis, proteins were transferred to polyvinylidene difluoride membranes (GE Healthcare, Buckinghamshire, United Kingdom). The blots were blocked with 4% ECL Advance Blocking Agent (GE Healthcare) in TBS/T buffer (20 mM Tris–HCl [pH 7.6], 137 mM NaCl, 0.1% Tween 20) for 2 h at room temperature. The blots were washed with TBS/T and incubated with primary antibodies overnight at 4°C. Goat anti-rabbit or goat anti-mouse peroxidase-conjugated secondary antibody was added to the membranes, which were then incubated for 1 h at room temperature. The protein bands on the membrane were visualized with SuperSignal West Femto Maximum Sensitivity Substrate (Thermo Fisher Scientific).

Transmission electron microscopy (TEM) analysis

RAW264.7 cells (3×10^5 cells/well) were seeded in 4-well Lab-Tek II Chambered Coverglass (Nunc), cultured at 37°C for 6 h, treated with 100 μg/mL nSP70, nSP70-C or medium (for negative control), and fixed in 2.5% glutaraldehyde and then in 1.5% osmium tetraoxide. The fixed cells were dehydrated and embedded in EPON resin. Ultrathin sections were stained with lead citrate and observed by transmission electron microscopy (HITACHI-H7650, HITACHI, Tokyo, Japan).

Assessment of in vivo inflammatory effects of silica particles

BALB/c mice were intraperitoneally injected with 1 mg of one type of silica particle in 200 μL phosphate-buffered saline (PBS) or PBS for negative control. Two or twenty-four hours after injection, the mice were sacrificed, and whole peritoneal cavity lavage fluid (PCLF) was collected using 4 mL of cooled PBS as previously described (Kops et al. 1986; Morishige et al. 2010a). Cytokine production patterns in the PCLF 2 h after injection were analyzed by means of a Mouse Cytokine 20-Plex Panel (Invitrogen, Carlsbad, CA) using a Bio-Plex Suspension Array System (Bio-Rad Laboratories, Tokyo, Japan). The total number of live cells in the PCLF 24 h after injection was determined with a Nucleo-Counter (Chemometec A/S, Allerød, Denmark).

Statistical analysis

All results are presented as means ± standard deviation (SD) or standard error of the mean (SEM). Differences were compared by using Student's t-tests or Scheffé's method after analysis of variance (ANOVA).

Results

Size dependence of silica particle-induced inflammatory responses

Here, we used nanosilica particles with diameters of 30 and 70 nm (nSP30 and nSP70, respectively) and conventional

microsilica particles with diameters of 300 and 1,000 nm (nSP300 and mSP1000, respectively). The hydrodynamic diameters of these particles, as measured by means of a dynamic light-scattering system, were 33, 78, 300, and 945 nm, respectively (Fig. 1a). The size distribution spectrum of each silica particle showed a single peak (Fig. 1a), and the hydrodynamic diameter corresponded almost precisely to the primary particle size for each sample, indicating that the silica particles used in this study were well-dispersed particles in solution. In addition, TEM images confirmed that the particles were well-dispersed smooth-surfaced spheres, as described previously (Yamashita et al. 2011). First, we assessed the correlation between the size of the silica particles and their inflammatory effects. We incubated RAW264.7 cells with each type of silica particle and measured TNFα production in the culture supernatant, because TNFα is a crucial modulator of inflammation (Fig. 1b). Of the various silica particles, nSP30 and nSP70 induced the highest TNFα production, whereas the larger nSP300 and mSP1000 did not induce such inflammatory responses.

Next, we assessed the correlation between particle size and inflammatory effects in vivo (Fig. 1c, d). We intraperitoneally injected silica particles into BALB/c mice and counted the total number of live cells in the PCLF, because inflammation is known to induce local infiltration of various inflammatory cells (Busuttil et al. 2004). We found that nSP30 and nSP70 induced significant cell migration compared with PBS, whereas nSP300 and mSP1000 showed low cell accumulation (Fig. 1c). Furthermore, we analyzed cytokine and chemokine production in the PCLF by using a cytokine array system (Fig. 1d). nSP30 and nSP70 induced greater production of interleukin-5 (IL-5) and IL-6, macrophage chemoattractant protein-1 (MCP-1), and keratinocyte chemoattractant (KC) than did nSP300 and mSP1000, although TNFα production was not detected in the PCLF. These results indicate that the nanosilica particles possessed a more potent inflammatory effect than did the larger silica particles.

Involvement of mitogen-activated protein kinases in nanosilica particle-induced inflammation

Mitogen-activated protein kinases (MAPKs) are a family of proteins, including p38, ERK, and JNK, that play key roles in regulation of the production of proinflammatory mediators and in apoptotic cell death (Jeffrey et al. 2007). To investigate the mechanisms of nanosilica particle-induced inflammation, we treated RAW264.7 cells with silica particles and used Western blotting analysis to examine the activation of MAPKs (Fig. 2a–c). We detected the phosphorylation of p38, ERK, and JNK in nSP30- and nSP70-treated cells. In contrast, little or no phosphorylation of
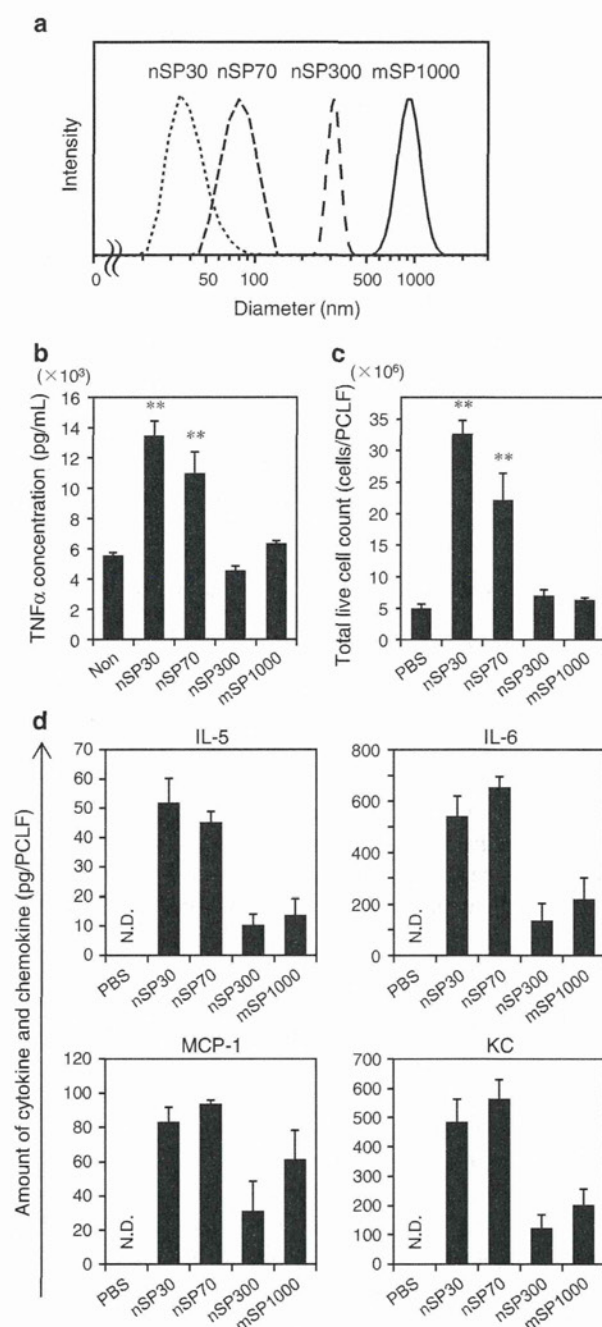

Fig. 1 Correlation between silica particle size and inflammatory effects in vitro and in vivo. **a** Size distribution of various sizes of silica particles was measured by a dynamic light-scattering method. **b** TNFα production levels in vitro. RAW264.7 cells were treated with each silica particle or no particles (Non) for 12 h, and then, TNFα production levels in the culture supernatants were measured. The data represent means ± SD ($n = 5$; **$P < 0.01$ versus value for medium control, ANOVA). **c, d** In vivo inflammatory effects. BALB/c mice were intraperitoneally injected with PBS or each silica particle; then, **c** the total number of live cells in the PCLF was counted after 24 h, and **d** cytokine and chemokine production in the PCLF was measured after 2 h. *N.D.* not detected. Data represent means ± SEM ($n = 5$; **$P < 0.01$ versus value for PBS control, ANOVA)
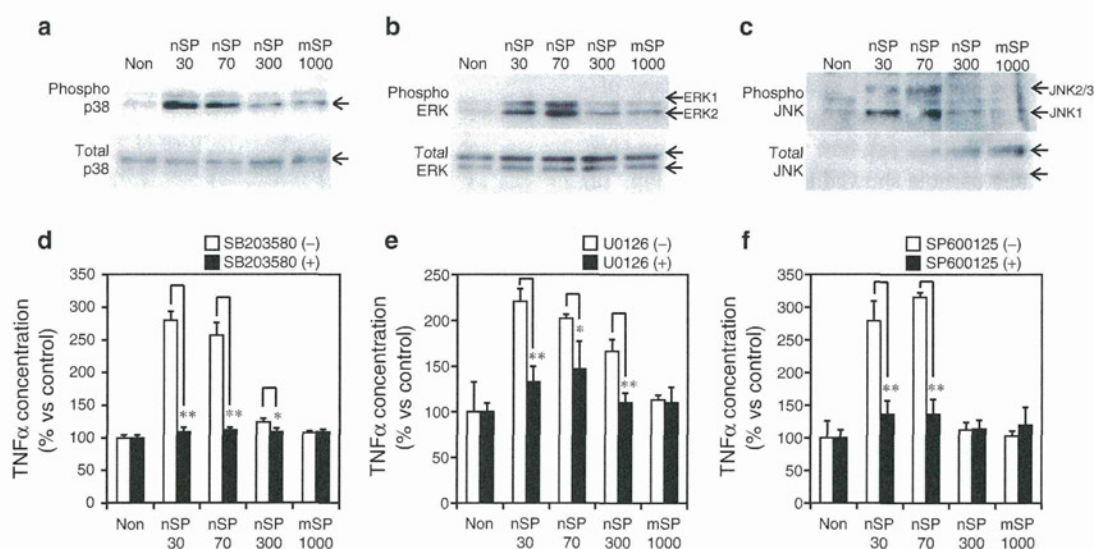
Fig. 2 Effects of silica particles on the activation of MAPKs. **a–c** Activation of MAPKs induced by silica particles. RAW264.7 cells were treated with silica particles of various sizes for 4 h. The whole-cell lysates were analyzed by Western blotting for phosphorylated and nonphosphorylated **a** p38, **b** ERK, and **c** JNK. **d–f** Association of MAPKs in silica particle-induced TNFα production.

RAW264.7 cells, pretreated with inhibitors of **d** p38, **e** ERK, or **f** JNK were exposed to silica particles, and 4 h after the treatment, TNFα production in the culture supernatants was measured. Dimethyl sulfoxide (0.1 %) was used as the control. Data represent means ± SD ($n = 5$; *$P < 0.05$, **$P < 0.01$ versus value for inhibitor [–] control within each treatment pair, t test)

MAPKs was detected in cells treated with nSP300 or mSP1000. No changes in the expression of nonphosphorylated p38, ERK, and JNK were observed in cells treated with silica particles. These results suggest that nanosilica particles might have induced inflammation via activation of MAPKs.

To confirm the importance of MAPKs in nanosilica particle-induced inflammation, we analyzed TNFα production in RAW264.7 cells treated with silica particles in the presence of an inhibitor of p38 (SB203580), ERK (U0126), or JNK (SP600125) (Fig. 2d–f). nSP30- and nSP70-induced TNFα production was almost completely suppressed by the inhibitors, indicating that nanosilica particle-induced TNFα production was mediated by MAPKs. Taken together, these results indicate that significant nanosilica particle-induced inflammation was mediated by the activation of MAPKs, whereas microsilica particles had little activation effect on MAPKs.

Involvement of the production of reactive oxygen species in nanosilica particle-induced inflammation

Intracellular reactive oxygen species (ROS) are reported to function as second messengers of inflammatory effects by activating multiple signaling pathways including a series of MAPKs (Bubici et al. 2006; Thannickal and Fanburg 2000). To investigate the involvement of ROS in nanosilica particle-induced TNFα production, we measured the TNFα concentrations induced by nSP30 and nSP70 in the presence BHA, a broad-spectrum ROS scavenger, or DPI, a specific inhibitor of NADPH oxidase, which is an important enzymatic producer of ROS (Morel et al. 1991). Both BHA and DPI significantly suppressed nanosilica particle-induced TNFα production (Fig. 3a, b), suggesting that nanosilica particle-induced production of ROS plays an important role in MAPK activation and subsequent inflammatory responses.

Suppression of inflammation by surface modification of nSP70

To investigate the influence of surface modification on nanosilica particle-induced inflammatory responses, we used nSP70 of which the surfaces had been modified with COOH groups (nSP70-C). We confirmed that nSP70-C were smooth-surfaced spherical particles by TEM as described previously (Yamashita et al. 2011). The mean secondary particle diameter of the nSP70-C was 70 nm, and the zeta potentials of nSP70 and nSP70-C were −53 and −76, respectively, indicating that surface modification changed the surface charge of the particles as described previously (Yamashita et al. 2011). We incubated RAW264.7 cells with nSP70 or nSP70-C for 12 h and then measured the TNFα concentrations. Whereas nSP70 induced high levels of TNFα production, nSP70-C induced low levels of TNFα production (Fig. 4a). Furthermore, we evaluated the inflammatory effects of nSP70 and nSP70-C in vivo. We intraperitoneally injected both types of particle separately into BALB/c mice
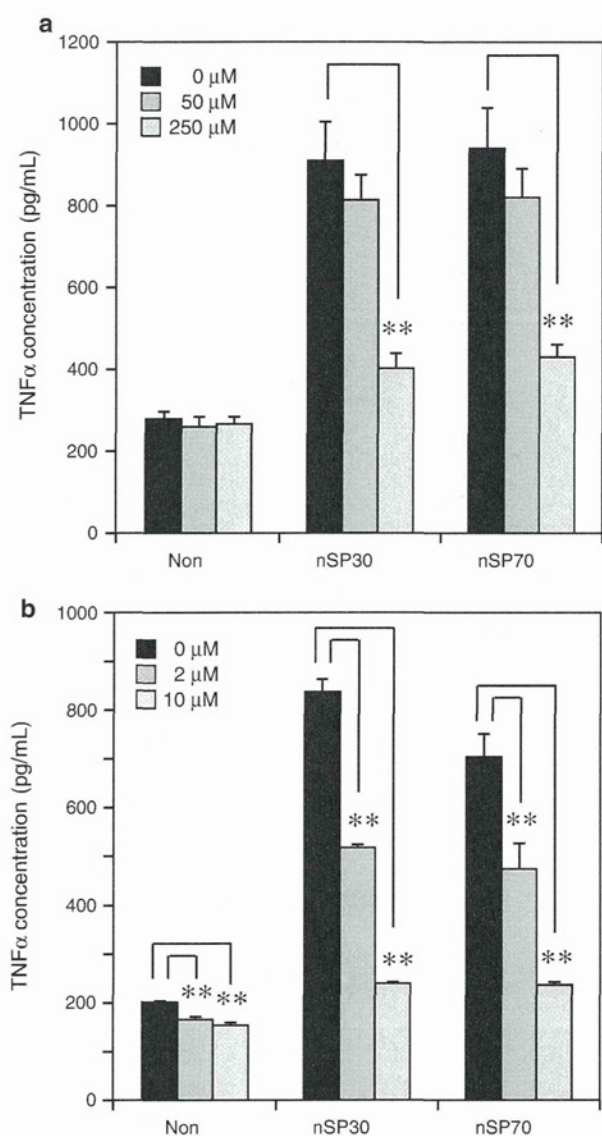
Fig. 3 Involvement of nanosilica particle-induced ROS production in TNFα production. RAW264.7 cells were treated with nSP30 or nSP70 for 4 h in the absence or presence of **a** BHA or **b** DPI at the indicated concentrations. TNFα production in the culture supernatants was measured. Data represent means ± SD ($n = 5$; **$P < 0.01$ versus value for inhibitor [−] control within each treatment pair, t test)

Fig. 4 Inflammatory responses induced by surface-modified nSP70. **a** TNFα production induced by nSP70 and nSP70-C. RAW264.7 cells were treated with nSP70 or nSP70-C for 12 h, and then, TNFα production in the culture supernatants was measured. Data represent means ± SD ($n = 5$; **$P < 0.01$ versus value for medium control, ††$P < 0.01$ versus value for nSP70, ANOVA). **b, c** In vivo inflammatory effects of nSP70 and nSP70-C. BALB/c mice were intraperitoneally injected with PBS or nSP70 or nSP70-C; **b** the total number of live cells in the PCLF was counted after 24 h, and **c** cytokine and chemokine production in the PCLF was measured after 2 h. *N.D.* not detected. Data represent means ± SEM ($n = 5$; **$P < 0.01$ versus value for PBS control, ††$P < 0.01$ versus value for nSP70, ANOVA)

and then counted the total number of live cells and measured the production of cytokines and chemokines in the PCLF. nSP70-C did not induce significant cell migration in treated mice, even though nSP70 induced strong inflammatory responses (Fig. 4b). In addition, cytokine and chemokine production in nSP70-C-treated mice was significantly lower than in nSP70-treated mice (Fig. 4c). We also confirmed that, in the 20-plex cytokine array system used in this study, there was no upregulation of cytokine and chemokine production in the nSP70-C-treated group (data not shown).
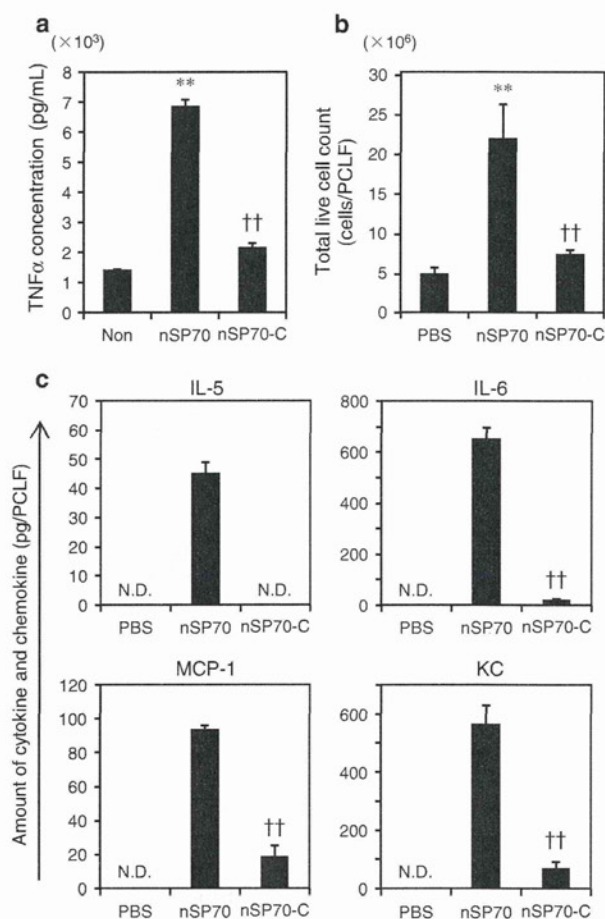
These results indicate that nSP70 modified with COOH groups are unlikely to induce undesired inflammatory responses.

Suppression of MAPK activation by surface modification of nSP70

Through their phagocytic activity, macrophages play an important role in determining the biopersistence of foreign particles and initiating inflammatory responses, including cytokine production. Therefore, we speculated that the reduction of inflammatory responses by surface modification of nSP70 resulted from a difference in the particle

Fig. 5 Effects of surface modification of nSP70 on the MAPKs pathway. **a** TEM analysis of nSP70 and nSP70-C. RAW264.7 cells were treated with nSP70 or nSP70-C for 4 h. Cells were then observed by TEM. **b** MAPK activation induced by nSP70 or nSP70-C. RAW264.7 cells were treated with nSP70 or nSP70-C for the indicated times. The whole-cell lysate was analyzed by Western blotting for phosphorylated and nonphosphorylated p38, ERK, and JNK
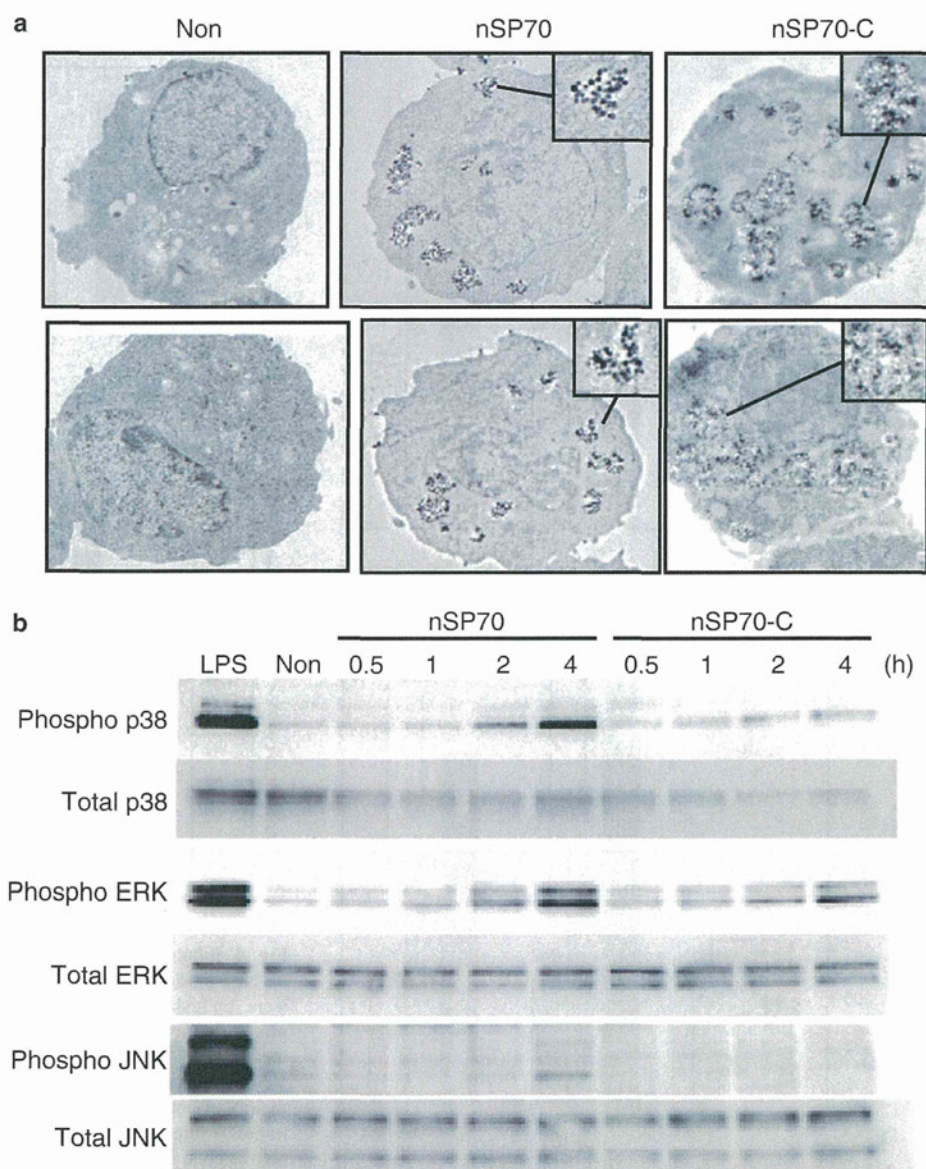
uptake frequency between the modified and unmodified nSP70. TEM analysis of the uptake frequency of nSP70-C clearly showed that they were taken up by RAW264.7 cells as well as nSP70 (Fig. 5a). Therefore, we attributed the difference between the inflammatory effects of the modified and unmodified particles to a difference in signaling intensity after ingestion of the particles into the cells. To elucidate the mechanisms by which surface modification suppressed the inflammatory effect of nSP70, we examined the activity of MAPKs in RAW264.7 cells treated with modified or unmodified nSP70 (Fig. 5b). nSP70-C induced low MAPK activation compared with nSP70 4 h after the treatment, although there was no noticeable difference at the time point of 0.5, 1, and 2 h after the treatment. Taken together, our observations suggest that surface modification

of nSP70 suppressed TNFα production by reducing nSP70-induced MAPK activation rather than by reducing cellular uptake frequency.

Cytotoxicity of silica particles

MAPKs are associated with cell growth, cell differentiation, and apoptotic cell death (Shiryaev and Moens 2010). Therefore, to investigate the influence of silica particle size on cytotoxicity, we treated RAW264.7 cells with silica particles of various sizes and examined the cell viability. nSP30 and nSP70 had significant cytotoxicity compared with the larger particles (nSP300 and mSP1000; Fig. 6a). To determine the impact of surface modification of the silica particles on cytotoxicity, we incubated RAW264.7
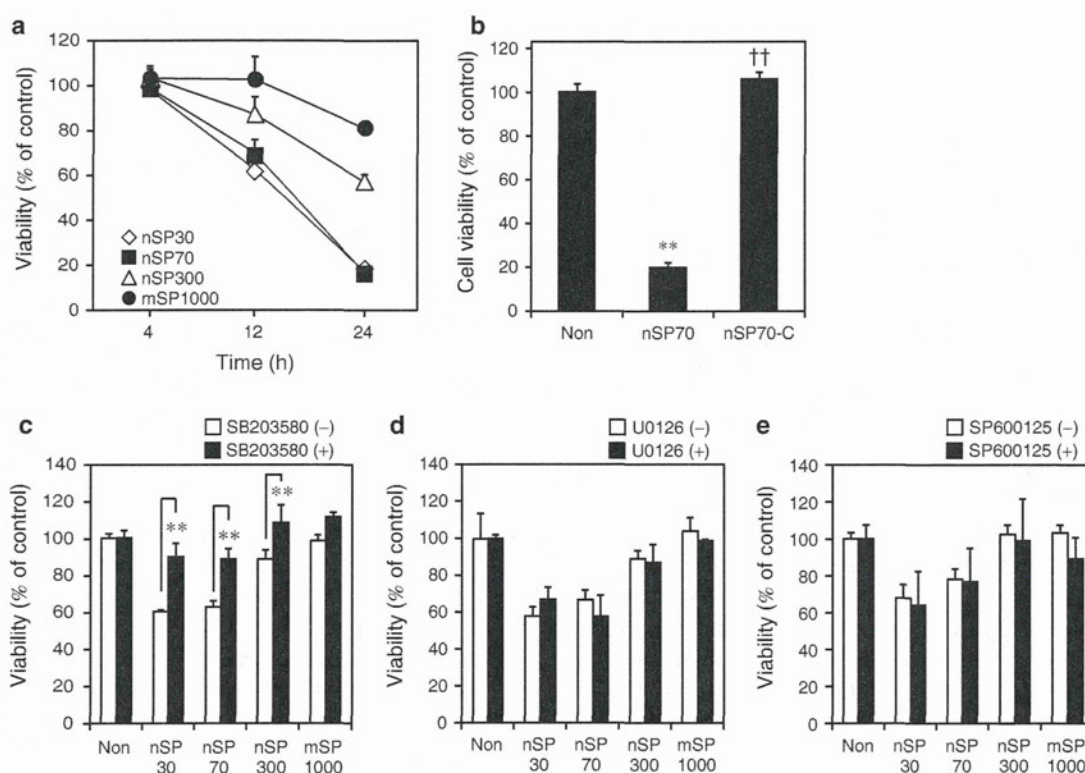
Fig. 6 Cytotoxicity induced by silica particles. **a** Cytotoxicity of silica particles. RAW264.7 cells were treated with silica particles of various sizes for the indicated time. Cell viability was assessed. Data represent means ± SD ($n = 5$). **b** Cytotoxicity of nSP70-C. RAW264.7 cells were treated with nSP70 or nSP70-C for 24 h. Cell viability was assessed. Data represent means ± SD ($n = 5$; **$P < 0.01$ versus value for medium control, ††$P < 0.01$ versus value for nSP70, ANOVA). **c–e** Association of MAPKs with silica particle-induced cell death. RAW264.7 cells pretreated with inhibitors of **c** p38 MAPK, **d** ERK, or **e** JNK were exposed to silica particles, and 12 h after the treatment, cell viability was assessed. Dimethyl sulfoxide (0.1%) was used as a control. Data represent means ± SD ($n = 5$; **$P < 0.01$ versus value for inhibitor [–] control within each treatment pair, t test)

cells with nSP70 and nSP70-C and again evaluated the cell viability. nSP70-C showed no cytotoxicity, whereas nSP70 induced significant cell death (Fig. 6b). We speculated that nanosilica particle-induced cell death depended on MAPK signaling triggered by nanosilica particles. Therefore, to investigate the association of MAPKs and nanosilica particle-induced cell death, we treated RAW264.7 cells with silica particles in the presence or absence of an inhibitor of p38 (SB203580), ERK (U0126), or JNK (SP600125). The p38 inhibitor (SB203580) significantly suppressed the cytotoxicity of nanosilica particles (Fig. 6c–e), whereas the inhibitors of ERK (U0126) and JNK (SP600125) did not. These findings indicate that nanosilica particle-induced cell death depended in part on p38, but was independent of ERK and JNK.

Discussion

We elucidated the effects of particle size and surface modification on silica particle-induced inflammatory responses, with the goal of obtaining basic information for use in the development of safe and effective nanomaterials. First, we evaluated the association between the size of silica particles and their inflammatory effects. We focused on TNFα production, because TNFα stimulates the acute-phase reaction and is involved in systemic inflammation. Furthermore, recent reports have shown that TNFα plays a critical role in the pathogenesis of silicosis (Li et al. 2009). We showed that nSP30 and nSP70 induced significant TNFα production in vitro, whereas nSP300 and mSP1000 exhibited low levels of TNFα production (Fig. 1b). In addition, we demonstrated that the nSP30 and nSP70 induced higher in vivo inflammatory responses than did nSP300 and mSP1000 (Fig. 1c, d). Among the most important sources of cytokines against inhaled foreign particles are macrophages, which are widely known as the first line of defense against such particles (Hornung et al. 2008). We attributed nanosilica particle-induced cytokine production to the inflammatory signaling cascade triggered by ingestion of the nanosilica particles by macrophages. Consistent with our consideration, the results obtained by

other studies indicate that smaller titanium dioxide particles induce strong inflammatory responses than do larger particles (Sager et al. 2008). Therefore, we suggest that investigation of the mechanisms of nanosilica particle-induced inflammation is necessary for the development of safe and effective nanosilica particles. Although nSP30 and nSP70 induced in vitro inflammatory responses, we did not detect the production of TNFα in vivo, perhaps owing to the timing of our measurement of TNFα production (Savici et al. 1994).

We also investigated the mechanisms of the inflammatory effects of nanosilica particles on RAW264.7 macrophages. Intracellular ROS function as second messengers of inflammatory effects by activating multiple signal pathways including a series of MAPKs (Thannickal and Fanburg 2000). The activation of MAPKs leads to the induction of transcription factors for TNFα production, such as nuclear factor κB, activator protein 1, and activating transcription factor (Bubici et al. 2006). These transcription factors control the inducible expression of genes of which the products are part of the inflammatory response. In fact, Ke et al. (2006) reported that ROS play an essential role in crystalline silica-induced TNFα production. Here, we demonstrated that smaller nanosilica particles activated MAPKs more strongly than did larger silica particles, and furthermore, we showed that nanosilica particle-induced intracellular ROS were important factors in nanosilica particle-induced inflammatory responses of macrophages (Figs. 2, 3). Consistent with our results, the recent results of Liu et al. showed that exposure to silica nanoparticles causes the generation of ROS in endothelial cells, which in turn induces endothelial apoptosis via JNK/p53 and evokes the activation of nuclear factor κB pathways (Liu and Sun 2010). These observations collectively suggest that nSP30- and nSP70-induced intracellular ROS may participate in the activation of MAPKs and subsequent inflammatory responses.

In contrast, our previous data showed that, by activating the cytoplasmic NOD-like receptor family member NLRP3 inflammasome, mSP1000 induce higher IL-1β production than do nanosilica particles (Morishige et al. 2010a). These results indicate that there are differences in the intracellular behavior, signaling pathways, and cytokine production profiles induced by silica particles of various sizes. Although the detailed mechanisms by which nano- and microsilica particles induce different signaling cascades remain unclear, recent reports have shown that nanomaterials are introduced into the macrophages via foreign-recognizing scavenger receptors rather than via the traditional endocytosis pathway (Iyer et al. 1996; Thakur et al. 2009). In particular, scavenger receptor class A-mediated recognition and ingestion of nanomaterials reportedly induce cytotoxicity and cytokine production via activation of p38

(Hirano et al. 2008; Limmon et al. 2008). Therefore, we speculate that the difference between the inflammatory effects of nano- and microsilica particles was due to differences in the pathways by which they are recognized and ingested.

We also examined the effect of surface modification on the inflammatory effects of silica particles, because particle surface properties have been demonstrated to be important factors for the particles' biological effects (Albrecht et al. 2004; He et al. 2008; Morishige et al. 2010a; Yamashita et al. 2011). Interestingly, although unmodified nSP70 and surface-modified nSP70-C were equally taken up, we found that nSP70-C did not induce inflammatory responses in vitro or in vivo (Figs. 4, 5a). Furthermore, nSP70-C induced less MAPK activation (Fig. 5b). These results indicate that changes in surface properties, such as the surface charge, suppressed the inflammatory responses induced by nSP70. We previously demonstrated that surface modification of mSP1000 with functional groups, including COOH groups, efficiently decreases mSP1000-induced ROS production (Morishige et al. 2010a). Therefore, we speculate that the nSP70-C triggered less ROS production (which induces TNFα production) than did unmodified nSP70, although more precise investigation is needed. It has recently been shown that nanomaterials become coated with serum proteins and induce different cellular responses by binding to proteins (Lesniak et al. 2010; Lundqvist et al. 2008). In addition, different surface characteristics, such as surface charge and surface functional groups, are known to influence the binding affinities of proteins to nanomaterials (Lundqvist et al. 2008). Therefore, the differences in protein binding between nSP70 and nSP70-C might have given rise to differences in the nanomaterials' inflammatory responses.

In addition to cytokine production, cell death induced by nanosilica particles is also a critical obstacle to the safety and efficacy of nanosilica particles, because macrophages play a central role in the defense system of the host. Our data indicate that nSP30 and nSP70 induced significant cell death and that their cytotoxicity might be dependent on p38 but independent of ERK and JNK signaling (Fig. 6). These results indicate that nanosilica particle-induced cell death depended on activation of p38, whereas nanosilica particle-induced production of TNFα was not involved in cell death. Consistent with these considerations, nSP70-C, which induces less MAPKs activation, did not trigger cell death.

We demonstrated that nanosilica particles induced stronger inflammatory responses than did microsilica particles and that nanosilica particle-induced TNFα production was mediated by the activation of ROS and MAPKs. Furthermore, by surface modification with COOH groups, we suppressed nanosilica particle-induced inflammatory responses by inhibiting the activation of MAPKs. We expect

that further studies of the relationship between surface characteristics and biological effects will provide useful information for the development of safe and effective nanomaterials.

Conflict of interest The authors declare that they have no competing interests.

References

Albrecht C, Schins RP, Hohr D, Becker A, Shi T, Knaapen AM et al (2004) Inflammatory time course after quartz instillation: role of tumor necrosis factor-alpha and particle surface. Am J Respir Cell Mol Biol 31:292–301

Bharali DJ, Klejbor I, Stachowiak EK, Dutta P, Roy I, Kaur N et al (2005) Organically modified silica nanoparticles: a nonviral vector for in vivo gene delivery and expression in the brain. Proc Natl Acad Sci USA 102:11539–11544

Bottini M, D'Annibale F, Magrini A, Cerignoli F, Arimura Y, Dawson MI et al (2007) Quantum dot-doped silica nanoparticles as probes for targeting of T-lymphocytes. Int J Nanomedicine 2:227–233

Bubici C, Papa S, Dean K, Franzoso G (2006) Mutual cross-talk between reactive oxygen species and nuclear factor-kappa B: molecular basis and biological significance. Oncogene 25:6731–6748

Busuttil SJ, Ploplis VA, Castellino FJ, Tang L, Eaton JW, Plow EF (2004) A central role for plasminogen in the inflammatory response to biomaterials. J Thromb Haemost 2:1798–1805

Chen Z, Meng H, Xing G, Yuan H, Zhao F, Liu R et al (2008) Age-related differences in pulmonary and cardiovascular responses to SiO2 nanoparticle inhalation: nanotoxicity has susceptible population. Environ Sci Technol 42:8985–8992

Decuzzi P, Godin B, Tanaka T, Lee SY, Chiappini C, Liu X et al (2010) Size and shape effects in the biodistribution of intravascularly injected particles. J Control Release 141:320–327

Dostert C, Petrilli V, Van Bruggen R, Steele C, Mossman BT, Tschopp J (2008) Innate immune activation through Nalp3 inflammasome sensing of asbestos and silica. Science 320:674–677

He X, Nie H, Wang K, Tan W, Wu X, Zhang P (2008) In vivo study of biodistribution and urinary excretion of surface-modified silica nanoparticles. Anal Chem 80:9597–9603

Hirano S, Kanno S, Furuyama A (2008) Multi-walled carbon nanotubes injure the plasma membrane of macrophages. Toxicol Appl Pharmacol 232:244–251

Hirsch LR, Stafford RJ, Bankson JA, Sershen SR, Rivera B, Price RE et al (2003) Nanoshell-mediated near-infrared thermal therapy of tumors under magnetic resonance guidance. Proc Natl Acad Sci USA 100:13549–13554

Hornung V, Bauernfeind F, Halle A, Samstad EO, Kono H, Rock KL et al (2008) Silica crystals and aluminum salts activate the NALP3 inflammasome through phagosomal destabilization. Nat Immunol 9:847–856

Huaux F (2007) New developments in the understanding of immunology in silicosis. Curr Opin Allergy Clin Immunol 7:168–173

Iyer R, Hamilton RF, Li L, Holian A (1996) Silica-induced apoptosis mediated via scavenger receptor in human alveolar macrophages. Toxicol Appl Pharmacol 141:84–92

Jeffrey KL, Camps M, Rommel C, Mackay CR (2007) Targeting dual-specificity phosphatases: manipulating MAP kinase signalling and immune responses. Nat Rev Drug Discov 6:391–403

Kagan VE, Bayir H, Shvedova AA (2005) Nanomedicine and nanotoxicology: two sides of the same coin. Nanomedicine 1:313–316

Ke Q, Li J, Ding J, Ding M, Wang L, Liu B et al (2006) Essential role of ROS-mediated NFAT activation in TNF-alpha induction by crystalline silica exposure. Am J Physiol Lung Cell Mol Physiol 291:L257–L264

Kops SK, Ratzlaff RE, Meade R, Iverson GM, Askenase PW (1986) Interaction of antigen-specific T cell factors with unique "receptors" on the surface of mast cells: demonstration in vitro by an indirect rosetting technique. J Immunol 136:4515–4524

Lesniak A, Campbell A, Monopoli MP, Lynch I, Salvati A, Dawson KA (2010) Serum heat inactivation affects protein corona composition and nanoparticle uptake. Biomaterials 31:9511–9518

Li X, Hu Y, Jin Z, Jiang H, Wen J (2009) Silica-induced TNF-alpha and TGF-beta1 expression in RAW264.7 cells are dependent on Src-ERK/AP-1 pathways. Toxicol Mech Methods 19:51–58

Limmon GV, Arredouani M, McCann KL, Corn Minor RA, Kobzik L, Imani F (2008) Scavenger receptor class-A is a novel cell surface receptor for double-stranded RNA. Faseb J 22:159–167

Liu X, Sun J (2010) Endothelial cells dysfunction induced by silica nanoparticles through oxidative stress via JNK/P53 and NF-kappaB pathways. Biomaterials 31:8198–8209

Lundqvist M, Stigler J, Elia G, Lynch I, Cedervall T, Dawson KA (2008) Nanoparticle size and surface properties determine the protein corona with possible implications for biological impacts. Proc Natl Acad Sci USA 105:14265–14270

Mantovani A, Allavena P, Sica A, Balkwill F (2008) Cancer-related inflammation. Nature 454:436–444

Mitchell LA, Lauer FT, Burchiel SW, McDonald JD (2009) Mechanisms for how inhaled multiwalled carbon nanotubes suppress systemic immune function in mice. Nat Nanotechnol 4:451–456

Morel F, Doussiere J, Vignais PV (1991) The superoxide-generating oxidase of phagocytic cells. Physiological, molecular and pathological aspects. Eur J Biochem 201:523–546

Morishige T, Yoshioka Y, Inakura H, Tanabe A, Yao X, Narimatsu S et al (2010a) The effect of surface modification of amorphous silica particles on NLRP3 inflammasome mediated IL-1beta production, ROS production and endosomal rupture. Biomaterials 31:6833–6842

Morishige T, Yoshioka Y, Tanabe A, Yao X, Tsunoda S, Tsutsumi Y et al (2010b) Titanium dioxide induces different levels of IL-1beta production dependent on its particle characteristics through caspase-1 activation mediated by reactive oxygen species and cathepsin B. Biochem Biophys Res Commun 392:160–165

Mossman BT, Churg A (1998) Mechanisms in the pathogenesis of asbestosis and silicosis. Am J Respir Crit Care Med 157:1666–1680

Nel A, Xia T, Madler L, Li N (2006) Toxic potential of materials at the nanolevel. Science 311:622–627

Poland CA, Duffin R, Kinloch I, Maynard A, Wallace WA, Seaton A et al (2008) Carbon nanotubes introduced into the abdominal cavity of mice show asbestos-like pathogenicity in a pilot study. Nat Nanotechnol 3:423–428

Roy I, Ohulchanskyy TY, Bharali DJ, Pudavar HE, Mistretta RA, Kaur N et al (2005) Optical tracking of organically modified silica nanoparticles as DNA carriers: a nonviral, nanomedicine approach for gene delivery. Proc Natl Acad Sci USA 102:279–284

Sager TM, Kommineni C, Castranova V (2008) Pulmonary response to intratracheal instillation of ultrafine versus fine titanium dioxide: role of particle surface area. Part Fibre Toxicol 5:17

Savici D, He B, Geist LJ, Monick MM, Hunninghake GW (1994) Silica increases tumor necrosis factor (TNF) production, in part, by upregulating the TNF promoter. Exp Lung Res 20:613–625

Shiryaev A, Moens U (2010) Mitogen-activated protein kinase p38 and MK2, MK3 and MK5: menage a trois or menage a quatre? Cell Signal 22:1185–1192

Takagi A, Hirose A, Nishimura T, Fukumori N, Ogata A, Ohashi N et al (2008) Induction of mesothelioma in p53± mouse by intraperitoneal application of multi-wall carbon nanotube. J Toxicol Sci 33:105–116

Thakur SA, Hamilton R Jr, Pikkarainen T, Holian A (2009) Differential binding of inorganic particles to MARCO. Toxicol Sci 107:238–246

Thannickal VJ, Fanburg BL (2000) Reactive oxygen species in cell signaling. Am J Physiol Lung Cell Mol Physiol 279:L1005–L1028

Verraedt E, Pendela M, Adams E, Hoogmartens J, Martens JA (2009) Controlled release of chlorhexidine from amorphous microporous silica. J Control Release 142:47–52

Waters KM, Masiello LM, Zangar RC, Tarasevich BJ, Karin NJ, Quesenberry RD et al (2009) Macrophage responses to silica nanoparticles are highly conserved across particle sizes. Toxicol Sci 107:553–569

Yamashita K, Yoshioka Y, Higashisaka K, Morishita Y, Yoshida T, Fujimura M et al (2010) Carbon nanotubes elicit DNA damage and inflammatory response relative to their size and shape. Inflammation 33:276–280

Yamashita K, Yoshioka Y, Higashisaka K, Mimura K, Morishita Y, Nozaki M et al (2011) Silica and titanium dioxide nanoparticles cause pregnancy complications in mice. Nat Nanotechnol 6:321–328

Yang X, Liu J, He H, Zhou L, Gong C, Wang X et al (2010) SiO2 nanoparticles induce cytotoxicity and protein expression alteration in HaCaT cells. Part Fibre Toxicol 7:1

Laboratory of Toxicology and Safety Science[1], Graduate School of Pharmaceutical Sciences, Osaka University; Laboratory of Biopharmaceutical Research[2], National Institute of Biomedical Innovation; The Center for Advanced Medical Engineering and Informatics[3], Osaka University, Osaka, Japan

Dermal absorption of amorphous nanosilica particles after topical exposure for three days

T. Hirai[1,2], T. Yoshikawa[1,2], H. Nabeshi[1,2], T. Yoshida[1,2], T. Akase[1,2], Y. Yoshioka[1,3], N. Itoh[1], Y. Tsutsumi[1,2,3]

The skin penetration and cellular localization of well-dispersed amorphous nanosilica particles (nSPs) with a diameter of 70 nm was analyzed in mice. Our results suggest that after topical exposure for three days the particles penetrate the skin barrier and are transported to the lymph nodes. These findings underscore the need to examine biological effects following dermal exposure to nSPs for the development of safer use of nSPs.

Nanomaterials (NMs) are defined as substances that have at least one dimension of less than 100 nm in size. NMs exhibit unique physicochemical properties that distinguish them from submicron-sized materials. These unusual properties have facilitated the development of innovative applications for NMs, which are already used in a wide variety of fields. For example, amorphous nanosilica particles (nSPs) and titanium dioxide nanoparticles (nTiO$_2$) are colorless and reflect ultraviolet light very effectively. Consequently, these substances are used in the cosmetics industry as a foundation and sunscreen (Lansdown and Taylor 1997; Napierska et al. 2010).

The reduced prticle size of NMs, however, poses new risks induced by changes in their biological reactivity and kinetics, which differ from those of bulk materials. For example, exposure of cells or animals to NMs, such as carbon nanotubes or nTiO$_2$, can induce cytotoxicity and inflammation that is different from that caused by exposure to submicron-sized materials (Nel et al. 2006; Xia et al. 2006). Furthermore, we have previously shown that nSPs display a different intracellular localization compared with submicron- or micro-sized silica particles, and induce a greater cytotoxic response. (Nabeshi et al. 2010; Yamashita et al. 2011; Nabeshi et al. in press) In general, risk is determined by the integrated value of a potential hazard with the amount of exposure. Hence, materials that are not absorbed and that have no effect on the application area pose no risk. Although there are a number of reports that focus on the biological response resulting from exposure to NMs, there is a paucity of information concerning the absorbency or localization of these materials. Thus, to accurately identify hazards associated with exposure to NMs, we must first analyze the *in vitro* and *in vivo* biodistribution of nSPs, especially with regard to penetration of biological barriers. Although we previously reported that topical application of nSP70 caused systemic exposure, absorbability of nSP70 after short term exposure has not yet been clarified.

In this study, we evaluated the intradermal absorption of well-dispersed nSPs with a particle size of 70 nm (nSP70) following topical exposure for three days. Specifically, nSP70 was applied to the inner side of the ears of female BALB/c mice for three days. The ears and regional lymph node were excised 24 h after the last administration and then analyzed by transmission electron microscopy. Our results show that nSP70 not only enter epidermal Langerhans cells, but also the cells in the dermis and regional lymph node.

Our findings suggest the particles can be dispersed throughout the body via the lymphatic transport system. Thus, exposure to nSPs in cosmetics poses an unknown risk that is not restricted to the application area. Hence, studies investigating the biological effects of dermal exposure to nSPs should include the whole body and not only the skin. Further studies are required to perform an appropriate risk analysis of nSPs e.g. quantitative determination of skin permeability and mechanisms for penetrating the skin barrier of nSP70. It is also important to investigate how nSPs behave after entering the body (e.g. accumulation potential, metabolism and excretion). Thus, we plan to collect ADME (absorption, distribution, metabolism and excretion) information as soon as possible. We believe that our study will provide useful information for developing safer NMs in the future.

Experimental

1. Silica particles

Suspensions of fluorescent (red-F)-labeled amorphous silica particles (Micromod Partikeltechnologie GmbH, Rostock, Germany) (25 mg/ml)
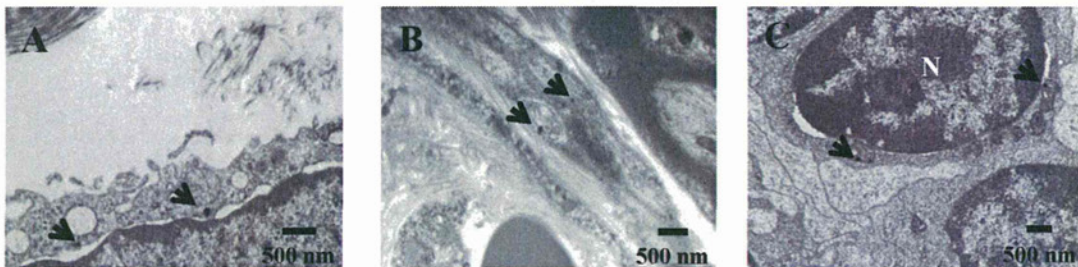

Fig.: Transdermal absorption test of nSP70 using the transmission electron microscopic (TEM) analysis. TEM analysis of skin and lymph node samples from mice after three-days of dermal exposure to nSP70. A-C, nSP70 (arrows) were present in the Langerhans cells (A), dermis (B) and cervical lymph node (C). N: nucleus. Scale bars: 500 nm (A–C)

were used in this study. Their particle diameter was 70 nm (nSP70). The suspensions of silica particles were sonicated for 5 min and then vortexed for 1 min immediately before use. Mean particle size was determined as described previously (Nabeshi et al. 2011), which confirmed that nSP70 remained as stable well-dispersed particles in water, rather than forming aggregates.

2. Dermal administration of silica particles and transmission electron microscopy analysis of skin and lymph node

nSP70 (250 mg/ear/day) were applied to the inner side of both ears of BALB/c mice for 3 days. Lymph nodes from each mouse were excised 24 h after the last administration of nSP70 and then fixed in 2.5% glutaraldehyde for 2 h. Small pieces of tissue sample were washed with phosphate buffer (three washes) and post-fixed in sodium cacodylate-buffered 1.5% osmium tetroxide for 60 min at 4 °C. The sample was block staining in 0.5% uranyl acetate and dehydrated by dipping through a series of solutions containing increasing concentrations of ethanol. Finally, the sample was embedded in Epon resin (TAAB). Ultrathin sections were stained with uranyl acetate and lead citrate. The stained samples were subsequently observed using a Hitachi electron microscope (H-7650; Hitachi, Tokyo, Japan).

References

Lansdown AB, Taylor A (1997) Zinc and titanium oxides: promising UV-absorbers but what influence do they have on the intact skin? Int J Cosmet Sci 19: 167–172.

Nabeshi H, Yoshikawa T, Matsuyama K, Nakazato Y, Arimori A, Isobe M, Tochigi S, Kondoh S, Hirai T, Akase T, Yamashita T, Yamashita K, Yoshida T, Nagano K, Abe Y, Yoshioka Y, Kamada H, Imazawa T, Itoh N, Tsunoda S, Tsutsumi Y (2010) Size-dependent cytotoxic effects of amorphous silica nanoparticles on Langerhans cells. Pharmazie 65: 199–201.

Nabeshi H, Yoshikawa T, Matsuyama K, Nakazato Y, Matsuo K, Arimori A, Isobe M, Tochigi S, Kondoh S, Hirai T, Akase T, Yamashita T, Yamashita K, Yoshida T, Nagano K, Abe Y, Yoshioka Y, Kamada H, Imazawa T, Itoh N, Nakagawa S, Mayumi T, Tsunoda S, Tsutsumi Y (2011) Systemic distribution, nuclear entry and cytotoxicity of amorphous nanosilica following topical application. Biomaterials 32: 2713–2724.

Nabeshi H, Yoshikawa T, Matsuyama K, Nakazato Y, Arimori A, Isobe M, Tochigi S, Kondoh S, Hirai T, Akase T, Yamashita T, Yamashita K, Yoshida T, Nagano K, Abe Y, Yoshioka Y, Kamada H, Imazawa T, Kondoh M, Yagi K, Mayumi T, Itoh N, Tsunoda S, Tsutsumi Y Well-dispersed amorphous nanosilicas induce fatal toxicity and consumptive coagulopathy after systemic exposure. Nanotechnol. 23: 045101.

Napierska D, Thomassen LC, Lison D, Martens JA, Hoet PH (2010) The nanosilica hazard: another variable entity. Part Fibre Toxicol 7: 39.

Nel A, Xia T, Madler L, Li N (2006) Toxic potential of materials at the nanolevel. Science 311: 622–627.

Xia T, Kovochich M, Brant J, Hotze M, Sempf J, Oberley T, Sioutas C, Yeh JI, Wiesner MR, Nel AE (2006) Comparison of the abilities of ambient and manufactured nanoparticles to induce cellular toxicity according to an oxidative stress paradigm. Nano Lett 6: 1794–1807.

Yamashita K, Yoshioka Y, Higashisaka K, Mimura K, Morishita Y, Nozaki M, Yoshida T, Ogura T, Nagano K, Abe Y, Kamada H, Imazawa T, Aoshima H, Kawai Y, Mayumi T, Tsunoda S, Itoh N, Yanagihara I, Saito S, Yoshikawa T, Tsutsumi Y (2011) Silica and titanium dioxide nanoparticles cause pregnancy complications in mice. Nat Nanotechnol 6: 321–328.

Laboratory of Toxicology and Safety Science[1], Graduate School of
Pharmaceutical Sciences, Osaka University; Laboratory of
Biopharmaceutical Research[2], National Institute of Biomedical Innovation,
The Center for Advanced Medical Engineering and Informatics[3], Osaka
University, Osaka, Japan

Amorphous nanosilica particles induce ROS generation in Langerhans cells

T. YOSHIDA[1,2], T. YOSHIKAWA[1,2], H. NABESHI[1,2],
K. MATSUYAMA[1,2], T. HIRAI[1,2], T. AKASE[1,2],
Y. YOSHIOKA[1,3], N. ITOH[1], Y. TSUTSUMI[1,2,3]

*Tomoaki Yoshikawa, Ph.D and Yasuo Tstsumi, Ph.D, Laboratory
of Toxicology and Safety Science, Graduate School of Pharmaceutical Sciences, Osaka University, 1-6 Yamadaoka, Suita,
Osaka 565-0871, Japan
tomoaki@phs.osaka-u.ac.jp, ytsutsumi@phs.osaka-u.ac.jp*

Generation of total intracellular reactive oxygen species (ROS) was measured in XS52 cells, a Langerhans cell-like line, treated with different sized amorphous silica particles. The results suggested that exposure to amorphous nanosilica particles (nSPs) with a particle size of 70 nm induced a higher level of ROS generation than did exposure to micron-sized amorphous silica particles. This finding means that it is essential to examine the biological effects of ROS generated after exposure to nSPs, which will provide useful information for hazard identification as well as the design of safer nanomaterials.

Recently, the development of nanomaterials (NMs) with particle sizes below 100 nm has received extensive interest. For example, titanium dioxide nanoparticles and amorphous nanosilica particles (nSPs) are colorless and reflect ultraviolet light more efficiency than micro-sized particles and have been already used in various applications such as cosmetics, medicines and foods (Fadeel et al. 2010). Thus, exposure to NMs is unavoidable for us in today's environment. In this respect, there is increasing concern regarding the potential health risks caused by exposure to NMs. In most cases, however, the evaluation of NMs has been insufficient for ensuring their safety. Hence, it is necessary to accumulate safety information, such as hazard data and exposure assessment to NMs, for risk evaluation to create safer forms of NMs.

Here, we have studied the relationship between the *in vivo/in vitro* distributions of NMs, together with their biological effects and physicality. In our previous study, we found that nSPs with particle size of 70 nm (nSP70) penetrated the stratum corneum of mice skin and were taken up by living cells such as keratinocytes and Langerhans cells after 28 days of exposure (Nabeshi et al. 2010). In another study, we showed that smaller sized amorphous silica particles induced greater cytotoxicity against XS52 cells, a Langerhans cell-like line (Nabeshi et al. 2009). Here, we have accumulated information to clarify amorphous silica particles-mediated cytotoxicity against XS52 cells in term of
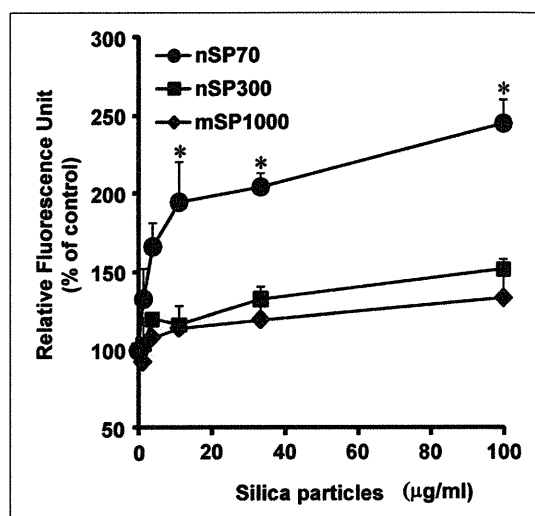

Fig.: Detection of ROS induced by silica particle treatment in XS52 cells. XS52 cells were incubated with various concentrations of nSP70 (circles), nSP300 (squares), and mSP1000 (diamonds) for 3 h. The total ROS induced by treatment with silica particles was expressed as relative fluorescence units in the DCFH assay. Data are presented as means $\pm$ SD (n = 4).*$P < 0.05$ versus the same dose of nSP300 or mSP1000

the levels of total intracellular reactive oxygen species (ROS) generated.

XS52 cells were treated with nSP70, and micro-sized amorphous silica particles with diameters of 300 or 1000 nm (nSP300 or mSP1000, respectively). As a result, all sizes of amorphous silica particles were found to induce intracellular ROS generation in a dose-dependent fashion. On the other hand, ROS generation by nSP70 treatment was significantly greater than that by nSP300 and mSP1000 treatment at the same particle concentration (Fig.). Thus, intracellular ROS generation in XS52 cells induced by amorphous silica particles was significantly increased by decreasing the particle size to less than 100 nm.

Some reports have indicated that ROS generation is related to a cellular stress response, such as DNA damage and apoptosis induction (D'Auteaux et al. 2007). The results of this study suggest that ROS generation may be involved in amorphous silica particles-mediated cytotoxicity in XS52 cells. In our previous study, we found that ROS generated by amorphous nanosilica particles induced DNA damage in human keratinocyte cells (Nabeshi et al. 2011). Therefore, these results suggest that DNA damage may be triggered by ROS induced by amorphous silica particles in XS52 cells. However, the detailed mechanism of NMs-mediated ROS generation remains unclear. Therefore, it is essential to analyze the mechanism underlying ROS generation induced by amorphous nanosilica particles to ensure the safety of NMs.

Recently, the mechanism of particulate matter-mediated ROS generation is gradually becoming clear. For example, it has been reported that inflammasomes are activated by actin-mediated endocytosis of crystalline silica or asbestos, which leads to NADPH oxidase activation and ROS generation (Dostert et al. 2008). Furthermore, many kinds of signaling pathways, such as Akt/P13K or MAPK pathways, are also related to ROS generation. On the basis of this information, we need to investigate whether these pathways are related to ROS generation induced by amorphous nanosilica particles. Furthermore, we should examine the relationship between physicality, exposure to amorphous silica particles and ROS generation. In the future, we

believe this information will be useful for the safety assessment and evaluation, as well as the design, of safer NMs.

1. Experimental

1.1. Silica particles

Suspensions of fluorescent (red-F)-labeled amorphous silica particles (Micromod Partikeltechnologie GmbH, Rostock, Germany) were used in this study; the particles had diameters of 70, 300, and 1000 nm (designated nSP70, nSP300, and mSP1000, respectively). The suspensions of silica particles were sonicated for 5 min and then vortexed for 1 min immediately prior to use.

1.2. Cell culture

Cells of the Langerhans cell-like line XS52 (a kind gift of Akira Takashima, University of Toledo, Health Science Campus, Toledo) were expanded in complete medium containing 2 ng/ml of murine GM-CSF and 10% culture supernatants from skin-derived stromal NS47 cells (a kind gift of Akira Takashima). The complete medium was RPMI-1640 medium supplemented with 10% heat-inactivated fetal calf serum, 1% non-essential amino acids, 1% L-glutamine, 1 mM sodium pyruvate, 1% 2-mercaptoethanol, 10 mM HEPES buffer, and 1% antibiotic-antimycotic mix stock solution.

1.3. Detection of reactive oxygen species (ROS)

Generation of total intracellular ROS was measured by monitoring the increasing fluorescence of 2'7'-dichlorofluprecein (DCF) using 2'7'-dichlorodihydorofluorecein diacetate (DCFH-DA; Sigma, St, Louis, MO). 3×10^4 XS52 cells were seeded into each well of a 96-well plate. After 24 h incubation, the cells were treated with nSP70, nSP300, or mSP1000 for 3 h. The cells were then washed once with phenol red-free medium, and incubated in 100 μl of DCFH-DA at 37 °C 5% CO_2 for 30 min. The fluorescence of DCF was monitored at the excitation and emission wave-length of 485 nm and 530 nm, respectively.

1.4. Statistical analysis

All data are reported as the mean ± SD. The significance of variation among different groups was determined by one-way ANOVA. Differences between the experimental group and the control group were determined by Williams' test. A value of $P < 0.05$ was considered significant.

References

D'Autreaux B, Toledano MB (2007) ROS as signalling molecles:mechanism that gerenate spefifity in ROS homeositasis. Nat Rev Cel Biol 8: 813–824.

Dostert C, Pétrilli V, Van Bruggen R, Steele C, Mossman BT, Tschopp J (2008) Innate immune activation through Nalp3 inflammasome sensing of asbestos and silica. Science 320: 674–677.

Fadeel B, Garcia-Bennett AE (2010) Better safe than sorry: Understanding the toxicological properties of inorganic nanoparticles manufactured for biomedical applications. Adv Drug Rev 62: 362–374.

Nabeshi H, Yoshikawa T, Matsuyama K, Nakazato Y, Arimori A, Isobe M, Tochigi S, Kondoh S, Hirai T, Akase T, Yamashita T, Yamashita K, Yoshida T, Nagano K, Abe Y, Yoshioka Y, Kamada H, Imazawa T, Itoh N, Tsunoda S, Tsutsumi Y (2010) Size-dependent cytotoxic effects of amorphous silica nanoparticles on Langerhans cells. Pharmazie 65: 199–201.

Nabeshi H, Yoshikawa T, Matsuyama K, Nakazato Y, Matsuo K, Arimori A, Isobe M, Tochigi S, Kondoh S, Hirai T, Akase T, Yamashita T, Yamashita K, Yoshida T, Nagano K, Abe Y, Yoshioka Y, Kamada H, Imazawa T, Itoh N, Nakagawa S, Mayumi T, Tsunoda S, Tsutsumi Y (2011) Systemic distribution, nuclear entry and cytotoxicity of amorphous nanosilica following topical application. Biomaterials 32: 2713–2724.

Laboratory of Toxicology and Safety Science[1], Graduate School of Pharmaceutical Sciences[2], Osaka University; Laboratory of Biopharmaceutical Research, National Institute of Biomedical Innovation; Osaka, Japan. Cancer Biology Research Center[3], Sanford Research/USD, Sioux Falls, SD, USA; The Center for Advanced Medical Engineering and Informatics[4], Osaka University, Osaka; Division of Foods[5], National Institute of Health Sciences, Tokyo, Japan

Potential of acute-phase proteins as biomarkers for sub-nano platinum exposure

T. Nagano[1,*], Y. Yoshioka[1,*], K. Higashisaka[1], A. Kunieda[1], K. Hata[1], K. Nagano[2], Y. Abe[3], H. Kamada[2,4], S. Tsunoda[2,4], H. Nabeshi[5], T. Yoshikawa[1], Y. Tsutsumi[1,2,4]

Yasuo Yoshioka, PhD, and Yasuo Tsutsumi, PhD, Laboratory of Toxicology and Safety Science, Graduate School of Pharmaceutical Sciences, Osaka University, 1-6 Yamadaoka, Suita, Osaka 565-0871, Japan
yasuo@phs.osaka-u.ac.jp, ytsutsumi@phs.osaka-u.ac.jp

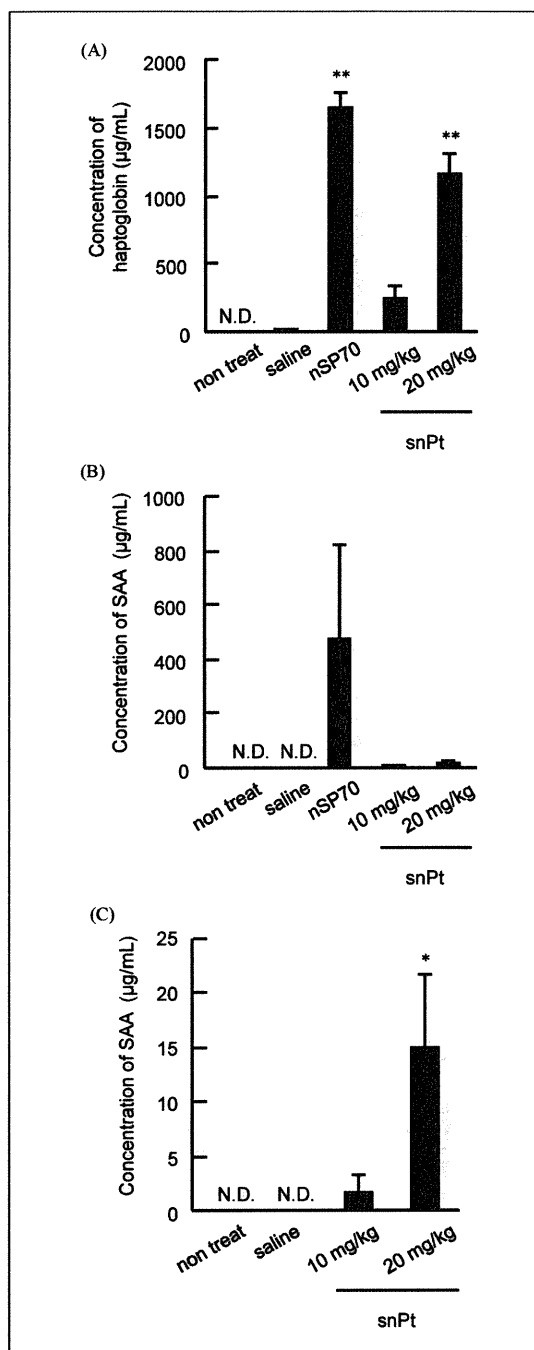*These authors contributed equally to this work.

Fig.: The potential of haptoglobin and serum amyloid A (SAA) as biomarkers of snPt. Female BALB/c mice were intravenously injected via the tail vein with sub-nano platinum (snPt), silica nanoparticles (nSP70), or saline, and blood samples were collected at 24 h after treatment. The serum levels of haptoglobin (A) and SAA (B) in each mouse were examined with ELISA. To clear the level of SAA in snPt-treated mice, the result of nSP70-treated mice was removed as shown in (C). Data are presented as mean ± SE. (n = 4–5; *$P < 0.05$, **$P < 0.01$ versus value for saline-treated group by ANOVA; N.D., not detected)

Recently, nanomaterials (NM) have been used in a range of different fields. However, their safety for human health is not yet sufficiently understood. Therefore, we attempted to establish a NM safety assessment system by focusing on biomarkers that may predict NM-induced adverse biological effects. We previously demonstrated that the acute-phase proteins haptoglobin and serum amyloid A (SAA) have potential as useful biomarkers of silica nanoparticle (nSP) exposure. Here, we investigated the potential of haptoglobin and SAA as biomarkers of sub-nano platinum (snPt) exposure. Serum levels of haptoglobin and SAA were measured in BALB/c mice by enzyme-linked immunosorbent assay. Serum levels of haptoglobin and SAA in snPt-treated mice were significantly higher than those of saline-treated mice. This suggests that haptoglobin and SAA have potential as biomarkers of snPt-induced adverse biological effects. These data provide useful information for the development of safe NM.

Nanomaterials (NM) are substances that have at least one dimension less than 100 nm. Compared with conventional materials of submicron size, NM possess innovative functions such as high electrical conductivity, tensile strength, and tissue permeability (Rutherglen and Burke 2009); they are now widely used in cosmetics, food, and medicines (Kaur and Agrawal 2007; Cormode et al. 2010). However, the increasing use of NM has resulted in public concern about their potential risks to health. In fact, there are various reports about adverse biological effects induced by NM (Hougaard et al. 2010; Morishige et al. 2010; Yamashita et al. 2011)_ENREF_8. It is therefore important to develop and promote safe NM because they have the potential to improve the quality of human life. We have tried to establish a NM safety assessment system that uses biomarkers. Biomarkers are expected to be useful not only in the detection of adverse biological responses, but also in the prediction of unknown biological effects induced by NM exposure (Casado et al. 2008). Biomarkers of NM will be invaluable for predicting potential toxicity

1

and establishing strategies for the development, production, and use of safe NM.

We previously demonstrated that haptoglobin and serum amyloid A (SAA) have potential as biomarkers for assessing biological responses to silica nanoparticle (nSP) exposure (Higashisaka et al. 2011). Sub-nano platinum (snPt) is already used in cosmetics and foods as an antioxidant agent (Onizawa et al. 2009), and it is expected to have therapeutic applications (Porcel et al. 2010). However, there are some concerns regarding adverse biological effects from snPt exposure (Park et al. 2010). Therefore, there is an urgent need to collect information about the safety of snPt.

Here, we investigated whether haptoglobin and SAA could be used as biomarkers of snPt. We used snPt with a diameter of 0.63 nm, and nSP with a diameter of 70 nm as a positive control. BALB/c mice were administered snPt (10 or 20 mg/kg), nSP (40 mg/kg), or saline via intravenous injection into the tail vein. We decided the dose of snPt by using previous data indicating that haptoglobin and SAA were significantly increased in mice treated with 40 mg/kg nSP (Higashisaka et al. 2011). Serum samples were collected at 24 h after administration and serum levels of haptoglobin and SAA were measured by enzyme-linked immunosorbent assay (ELISA). Serum levels of haptoglobin and SAA in snPt-treated mice were significantly higher than those of saline-treated mice (Fig.). In addition, although the levels of haptoglobin were almost the same in snPt-treated and nSP-treated mice, the levels of SAA were quite different (Fig.). Our results suggest that haptoglobin and SAA are potential biomarkers of snPt and that differences in biological effects are dependent on the type of NM.

Exposure to snPt in daily life can occur through various different routes. For example, snPt contained in food is taken up orally, whereas snPt within the manufacturing environment generally enters the body intranasally. Therefore, the evaluation of biomarkers for oral or intranasal exposure to snPt is also needed. We are now trying to evaluate why SAA showed different expression in snPt-treated and nSP-treated mice. We expect that this study will provide useful information for the development of biomarkers of NM exposure. We believe that the establishment of a NM safety assessment system based on biomarkers will lead to the development of safe NM.

Experimental

1. Materials

snPt and nSP were purchased from Polytech & Net GmbH (Schwalbach, Germany) and Micromod Partikeltechnologie (Rostock/Warnemünde, Germany), respectively. They were sonicated for 5 min and then vortexed for 1 min prior to use.

2. Animals

Female BALB/c mice were purchased from Nippon SLC, Inc. (Shizuoka, Japan) and used at 6 to 7 weeks of age. All of the animal experimental procedures in this study were performed in accordance with the Osaka University and the National Institute of Biomedical Innovation guidelines for the welfare of animals.

3. Blood-sample collection

BALB/c mice were administered snPt (10 or 20 mg/kg), nSP (40 mg/kg), or saline via intravenous injection into the tail vein. Blood samples were collected at 24 h after treatment, and serum was harvested by centrifugation at 8000 g for 15 min.

### 4. Measurement of acute-phase proteins

Serum levels of haptoglobin and SAA were measured with commercial ELISA kits (Life Diagnostics, Inc.; West Chester, PA) according to the manufacturer's instructions.

5. Statistical analyses

All results are expressed as means ± SE. Differences were compared by using the Bonferroni method after analysis of variance (ANOVA).

References

Casado B, Iadarola P, Luisetti M, Kussmann M (2008) Proteomics-based diagnosis of chronic obstructive pulmonary disease: the hunt for new markers. Expert Rev Proteomics 5: 693–704.

Cormode DP, Jarzyna PA, Mulder WJ, Fayad ZA (2010) Modified natural nanoparticles as contrast agents for medical imaging. Adv Drug Deliv Rev 62: 329–338.

Higashisaka K, Yoshioka Y, Yamashita K, Morishita Y, Fujimura M, Nabeshi H, Nagano K, Abe Y, Kamada H, Tsunoda S, Yoshikawa T, Itoh N, Tsutsumi Y (2011) Acute phase proteins as biomarkers for predicting the exposure and toxicity of nanomaterials. Biomaterials 32: 3–9.

Hougaard KS, Jackson P, Jensen KA, Sloth JJ, Loschner K, Larsen EH, Birkedal RK, Vibenholt A, Boisen AM, Wallin H, Vogel U (2010) Effects of prenatal exposure to surface-coated nanosized titanium dioxide (UV-Titan). A study in mice. Part Fibre Toxicol 7: 16.

Kaur IP, Agrawal R (2007) Nanotechnology: a new paradigm in cosmeceuticals. Recent Pat Drug Deliv Formul 1: 171–182.

Morishige T, Yoshioka Y, Tanabe A, Yao X, Tsunoda S, Tsutsumi Y, Mukai Y, Okada N, Nakagawa S (2010) Titanium dioxide induces different levels of IL-1beta production dependent on its particle characteristics through caspase-1 activation mediated by reactive oxygen species and cathepsin B. Biochem Biophys Res Commun 392: 160–165.

Onizawa S, Aoshiba K, Kajita M, Miyamoto Y, Nagai A (2009) Platinum nanoparticle antioxidants inhibit pulmonary inflammation in mice exposed to cigarette smoke. Pulm Pharmacol Ther 22: 340–349.

Park EJ, Kim H, Kim Y, Park K (2010) Intratracheal instillation of platinum nanoparticles may induce inflammatory responses in mice. Arch Pharm Res 33: 727–735.

Porcel E, Liehn S, Remita H, Usami N, Kobayashi K, Furusawa Y, Le Sech C, Lacombe S (2010) Platinum nanoparticles: a promising material for future cancer therapy? Nanotechnology 21: 85103.

Rutherglen C, Burke P (2009) Nanoelectromagnetics: circuit and electromagnetic properties of carbon nanotubes. Small 5: 884–906.

Yamashita K, Yoshioka Y, Higashisaka K, Mimura K, Morishita Y, Nozaki M, Yoshida T, Ogura T, Nabeshi H, Nagano K, Abe Y, Kamada H, Monobe Y, Imazawa T, Aoshima H, Shishido K, Kawai Y, Mayumi T, Tsunoda S, Itoh N, Yoshikawa T, Yanagihara I, Saito S, Tsutsumi Y (2011) Silica and titanium dioxide nanoparticles cause pregnancy complications in mice. Nat Nanotechnol 6: 321–328.
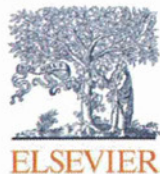
Amorphous silica nanoparticles enhance cross-presentation in murine dendritic cells

Toshiro Hirai [a], Yasuo Yoshioka [a,*], Hideki Takahashi [a], Ko-ichi Ichihashi [a], Tokuyuki Yoshida [a], Saeko Tochigi [a], Kazuya Nagano [b], Yasuhiro Abe [c], Haruhiko Kamada [b,d], Shin-ichi Tsunoda [b,d], Hiromi Nabeshi [e], Tomoaki Yoshikawa [a], Yasuo Tsutsumi [a,b,d,*]

[a] Laboratory of Toxicology and Safety Science, Graduate School of Pharmaceutical Sciences, Osaka University, 1-6 Yamadaoka, Suita, Osaka 565-0871, Japan
[b] Laboratory of Biopharmaceutical Research, National Institute of Biomedical Innovation, 7-6-8 Saitoasagi, Ibaraki, Osaka 567-0085, Japan
[c] Cancer Biology Research Center, Sanford Research/USD, 2301 E. 60th Street N, Sioux Falls, SD 57104, USA
[d] The Center for Advanced Medical Engineering and Informatics, Osaka University, 1-6 Yamadaoka, Suita, Osaka 565-0871, Japan
[e] Division of Foods, National Institute of Health Sciences, 1-18-1 Kamiyoga, Setagaya-ku, Tokyo 158-8501, Japan

ARTICLE INFO

ABSTRACT

Nanomaterials (NMs) exhibit unique physicochemical properties and innovative functions, and they are increasingly being used in a wide variety of fields. Ensuring the safety of NMs is now an urgent task. Recently, we reported that amorphous silica nanoparticles (nSPs), one of the most widely used NMs, enhance antigen-specific cellular immune responses and may therefore aggravate immune diseases. Thus, to ensure the design of safer nSPs, investigations into the effect of nSPs on antigen presentation in dendritic cells, which are central orchestrators of the adaptive immune response, are now needed. Here, we show that nSPs with diameters of 70 and 100 nm enhanced exogenous antigen entry into the cytosol from endosomes and induced cross-presentation, whereas submicron-sized silica particles (>100 nm) did not. Furthermore, we show that surface modification of nSPs suppressed cross-presentation. Although further studies are required to investigate whether surface-modified nSPs suppress immune-modulating effects in vivo, the current results indicate that appropriate regulation of the characteristics of nSPs, such as size and surface properties, will be critical for the design of safer nSPs.

© 2012 Elsevier Inc. All rights reserved.

1. Introduction

Nanomaterials (NMs) are substances that have at least one external dimension ⩽100 nm. Due to their small size and large surface-to-volume ratio, NMs show properties that are not found in bulk samples of the same material (particle size >100 nm) such as tissue permeability and biologic reactivity [1,2]. Thus, over the last decade, the use of NMs has increased in products such as cosmetics, foods, and medicines as a way of adding value to new or existing products [3–5].

However, there is now worldwide concern over whether the novel properties of NMs make them unsafe for humans. For example, it has been reported that titanium dioxide nanoparticles

(nTiO$_2$) induce DNA damage and genetic instability in vivo [6]. Furthermore, we have shown that nTiO$_2$ and amorphous silica nanoparticles (nSPs) induce reproductive toxicity and consumptive coagulopathy in mice [7,8]. Despite intensive research efforts, the relationships between biological responses to and the physicochemical properties of NMs, such as their size and surface properties, are not yet well understood. To fully utilize the potential benefits of NMs, it is crucial that we obtain more information for the design of safer NMs.

Previously, we showed that nSPs—one of the most frequently used NMs in cosmetics and foods [9]—with a diameter of 70 nm (nSP70) penetrate the skin barrier and enter dendritic cells (DCs) in the skin in mice [10,11]. Because DCs are central orchestrators of immunity that provide necessary innate signals and adaptive functions through the processing and presentation of antigens to which T cells respond [12,13], it is possible that nSPs have immune-modulating effects and are associated with the development of immune diseases. We further showed that co-administration of nSPs plus protein-antigen enhances antigen-specific CD8$^+$ T cell response and aggravates immune diseases in mice [14,15]. CD8$^+$ T cell response is only activated if

antigen-presenting cells, mainly DCs, present antigens on their major histocompatibility complex (MHC) class I molecules [16]. However, most exogenous antigens, which are introduced into DCs by the endocytic pathway, are not presented on MHC class I molecules [17]; most exogenous antigens are presented on MHC class II molecules [18]. Because nSPs enhance the CD8+ T cell response against exogenous antigen, nSPs might affect antigen processing and presentation in DCs. We hypothesize that nSPs promote the presentation of exogenous antigen on MHC class I molecules, through a pathway termed cross-presentation, which subsequently induces an immune-modulating effect.

Here, we investigate the influence of nSPs on antigen presentation via cross-presentation in DCs.

2. Materials and methods

2.1. Silica particles

Unmodified amorphous silica particles (SPs) with diameters of 70, 100, 300, or 1000 nm (designated nSP70, nSP100, nSP300, and mSP1000, respectively) and nSP70 modified with surface carboxyl groups (nSP70-C) or amine groups (nSP70-N) were purchased from Micromod Partikeltechnologie (Rostock/Warnemünde, Germany). Silica particle suspensions were stored at room temperature. The suspensions were sonicated and then vortexed for 1 min immediately prior to use. The physicochemical properties of these SPs have been described previously [10,15,19].

2.2. Regents

Polyinosinic acid (Poly I), chloroquine, and lactacystin were purchased from Sigma–Aldrich (St. Louis, MO, USA).

2.3. Cell culture

DC2.4 cells, which were previously characterized as immature DC cells from C57BL/6 (H-2 Kb) [20], were kindly provided by Dr. Kenneth L. Rock (Department of Pathology, University of Massachusetts Medical School, Worcester, MA, USA) and maintained in RPMI-1640 medium (Wako, Osaka, Japan) supplemented with 10% FBS, 10 ml/L 100× nonessential amino acid solution (Gibco, Invitrogen, Carlsbad, CA, USA), 50 μM 2-mercaptoethanol (Gibco), and 1% antibiotic cocktail (Nacalai Tesque, Kyoto, Japan). CD8-OVA1.3 cells, a T–T hybridoma against the OVA$_{257-264}$/MHC class I molecule (H-2 Kb) complex [21], were kindly provided by Dr. Clifford V. Harding (Case Western Reserve University, Cleveland, OH, USA) and maintained in Dulbecco's modified Eagle's medium (D-MEM; Wako) supplemented with 10% FBS, 50 μM 2-mercaptoethanol, and antibiotics cocktail. Cell viability was determined by using a WST-8 assay kit (Nacalai Tesque).

2.4. Cross-presentation assay

DC2.4 cells were seeded at a density of 5×10^4 cells/well in a 96-well flat-bottom culture plate (Nunc, Roskilde, Denmark) and incubated overnight at 37 °C (95% room air, 5% CO$_2$). Each well was then washed with PBS and the cells pulsed with 2.9–15 μg/mL of one of the silica particle suspensions and 100 μg/mL chicken egg ovalbumin (OVA; Sigma–Aldrich), or 100 μg/mL OVA alone. After 24 h, each well was washed with PBS and the cells fixed with 0.05% glutaraldehyde (Wako). The cells were then co-cultured with 1×10^5 cells/well of CD8-OVA1.3 cells for 24 h. The amount of interleukin 2 (IL-2) released into an aliquot of culture medium (200 μL) was measured by using a murine IL-2 ELISA kit

(eBioscience, San Diego, CA, USA) according to the manufacturer's instructions.

To study the antigen presentation pathway, DC2.4 cells (5×10^4 cells/well) were incubated with 100 μg/mL Poly I, 50 μM chloroquine, or 2.5 μM lactacystin for 1 h prior to the addition of OVA and one of the nSPs. In these assays, because the inhibitors are cytotoxic, we pulsed the cells with nSP70 (40 μg/mL) and OVA (100 μg/mL) in the continued presence of inhibitor for only 6 h. After incubation, the cells were washed and fixed, and 1×10^5 cells/well of CD8-OVA1.3 cells was added. After 24 h, the IL-2 levels in the supernatants were measured as described above.

2.5. Statistical analysis

All data are presented as mean ± SD. Differences were compared by using Student's t-test or Dunnett's test after ANOVA. Differences between the experimental groups and the control group were considered significant at $P < 0.05$.

3. Results and discussion

3.1. nSPs enhance cross-presentation

Here, we used nSPs with diameters of 70 and 100 nm (nSP70 and nSP100, respectively) and conventional SPs with diameters of 300 and 1000 nm (nSP300 and mSP1000, respectively). We previously confirmed that the hydrodynamic diameters of these particles, as measured by means of a dynamic light scattering system, were 76, 106, 264, and 1136 nm, respectively [15]. The size distribution spectrum of each silica particle showed a single peak and the hydrodynamic diameter corresponded almost exactly to the primary particle size for each sample, indicating that the silica particles used in this study are well-dispersed in solution [10,15]. In addition, transmission electron microscopy (TEM) images confirmed that the particles are well-dispersed smooth-surfaced spheres, as described previously [10].

To examine whether nSPs affect antigen processing and presentation in DCs and enhance cross-presentation, we first assessed the correlation between particle size and cross-presentation. DC2.4 cells were incubated with the SPs and OVA, and then co-cultured with CD8-OVA1.3 cells. When CD8-OVA1.3 cells recognize OVA$_{257-264}$/H-2 Kb complexes and become stimulated, they begin to produce IL-2. The amount of IL-2 in the supernatant correlates with the frequency of OVA presentation on MHC class I molecules; therefore, we assessed the cross-presentation of OVA by determining the amount of IL-2 released into an aliquot of culture medium. IL-2 production in the nSP70- and nSP100-treated groups was increased in a dose-dependent manner and was significantly higher than that in the OVA alone group (Fig. 1). In contrast, IL-2 production in the nSP300- and mSP1000-treated groups was the same as that in the OVA alone group (Fig. 1). These results suggest that nSPs influence antigen processing and induce cross-presentation in DCs.

3.2. nSP70 induces cross-presentation via the cytosolic pathway and is dependent on nSP70 uptake via scavenger receptors

There are two main intracellular pathways of cross-presentation: the cytosolic pathway and the vacuolar pathway [16,22,23]. In cross-presentation via the cytosolic pathway, internalized antigens enter the cytosol via endosomes, which are then degraded by proteasomes. Proteasome-generated peptides then feed into the classical MHC class I-mediated antigen presentation pathway in the same way as endogenous antigens. In contrast, in the vacuolar pathway, antigens are degraded within
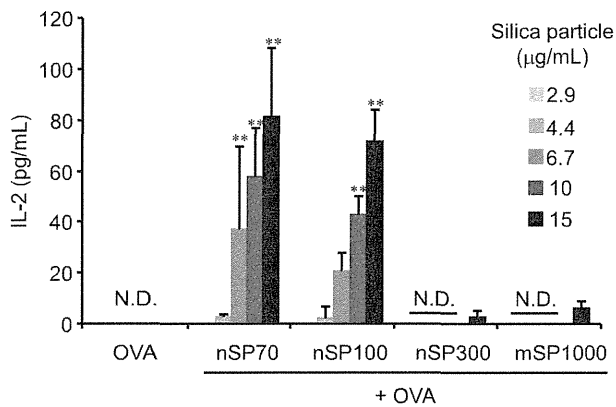
Fig. 1. The effect of different-sized silica particles on OVA presentation on MHC class I molecules in DC2.4 cells. DC2.4 cells were pulsed with OVA alone or OVA plus one of the sizes of silica. After silica exposure, the DC2.4 cells were co-cultured with CD8-OVA1.3 cells. The concentration of IL-2 in the supernatants was measured. The data are presented as the mean ± SD for three independent cultures (n = 3). N.D. not detected. **$P < 0.01$ versus OVA alone group by Dunnett's test.

the endosomes through endosomal acidification, and both antigen processing and loading onto MHC class I molecules occur within endocytic compartments. To determine which pathway is involved in nSP70-induced cross-presentation, we examined the effect of the potent proteasome inhibitor lactacystin or the endosomal acidification inhibitor chloroquine on nSP70-induced cross-presentation. Chloroquine treatment did not inhibit nSP70-induced IL-2 production (Fig. 2A), whereas lactacystin treatment strongly inhibited nSP70-induced IL-2 production (Fig. 2B). These results suggest that nSP70 induces cross-presentation via the cytosolic pathway.

Next, we analyzed the effect of cellular uptake of nSP70 on the induction of cross-presentation. Because some reports have shown that scavenger receptors (SRs) are related to the uptake of crystalline silica particles and nSPs [24,25], we examined nSP70-induced cross-presentation after treatment with Poly I, which is an SR inhibitor. nSP70-induced cross-presentation was completely inhibited by treatment with Poly I (Fig. 2C); therefore, nSP70-induced cross-presentation is dependent on SRs.

3.3. Effect of nSP70 surface modification on cross-presentation

Recent articles have focused on the possible influence of surface charge on the in vivo biodistribution, cellular uptake, and/or cytotoxicity of nanoparticles [7,26,27]. Taken together, these studies have shown that the surface properties of nSPs could be important for the development of safer nSPs. To investigate the effect of surface modification of nSP70 on cross-presentation, we evaluated cross-presentation in DC2.4 cells treated with OVA and nSP70 modified with either surface amine groups (nSP70-N) or carboxyl groups (nSP70-C). As mentioned above, we confirmed through TEM that nSP70-N and nSP70-C are smooth-surfaced, spherical particles, and that surface modification changes the surface charge of the particles [7]. IL-2 production in the OVA and nSP70-N- or nSP70-C-treated groups was not enhanced compared with the OVA only group; however, it was enhanced in the OVA and nSP70-treated group (Fig. 3). These results indicate that nSPs modified with surface amine groups or carboxyl groups do not induce
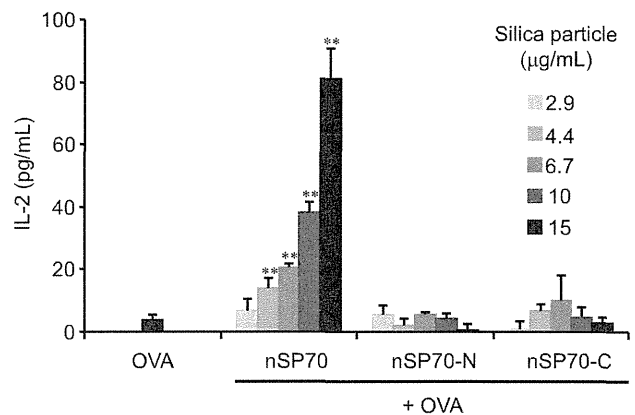

Fig. 3. Relationship between the surface physicochemical properties of nSP70 and nSP70-induced cross-presentation. DC2.4 cells were pulsed with OVA alone or OVA plus one of the nSP70s. After silica exposure, the DC2.4 cells were co-cultured with CD8-OVA1.3 cells for 24 h. The concentration of IL-2 in the supernatants was measured. The data are presented as the mean ± SD for three independent cultures (n = 3). **$P < 0.01$ versus OVA alone group by Dunnett's test.
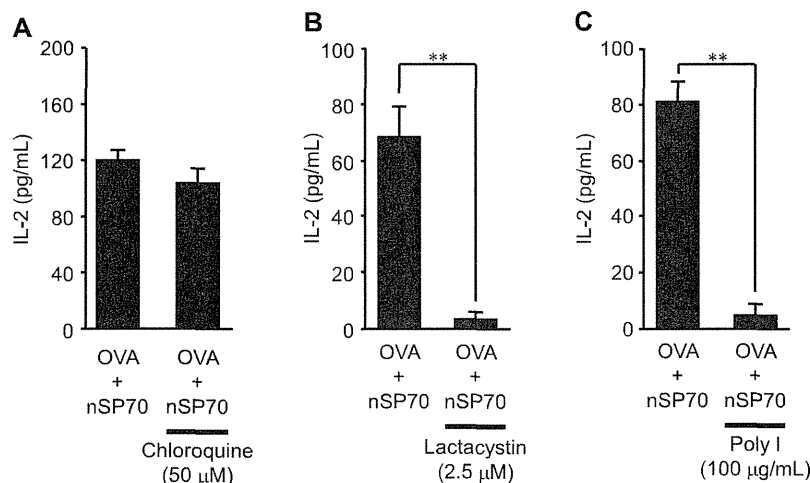

Fig. 2. Effects of various inhibitors on nSP70-induced cross-presentation. DC2.4 cells were pretreated with or without 50 μM chloroquine (A), 2.5 μM lactacystin (B), or 100 μg/mL Poly I (C). After 1-h incubation, DC2.4 cells were pulsed with OVA alone or OVA plus nSP70. After nSP70 exposure, DC2.4 cells were co-cultured with CD8-OVA1.3 cells. The concentration of IL-2 in the supernatants was measured. The data are presented as the mean ± SD for three independent cultures (n = 3). **$P < 0.01$ versus OVA alone group by Student's t-test.

cross-presentation. Therefore, appropriate regulation of the surface properties of nSPs may produce safer nSPs that do not induce cross-presentation and immune-modulation.

It is important to clarify why nSP70 induces cross-presentation yet nSP70-N and nSP70-C do not. It has been reported that the production of reactive oxygen species (ROS) induces the rupturing of endosomal/lysosomal membranes [28,29]. We previously reported that nSPs with a diameter $\leqslant$ 100 nm strongly induce endocytosis-dependent ROS generation [30]. It is therefore possible that nSP70 induces ROS generation dependent on SRs, which causes phagosomal destabilization and subsequently more antigen enters the cytosol. Furthermore, we observed that in the murine macrophage cell line Raw264.7, nSP70-N and nSP70-C induce little ROS production compared with nSP70 (data not shown). Although further analysis of the relationship between ROS production and nSP-induced cross-presentation is needed, it is possible that only unmodified nSPs induce ROS production and enhance cross-presentation.

In the current study, we showed that nSPs with diameters between 70 and 100 nm enhance cross-presentation. Furthermore, we showed that surface modification of nSPs with amine or carboxyl groups results in little cross-presentation. Although further studies are required to investigate whether surface modification of nSPs suppresses immune-modulating effects *in vivo*, these results indicate that appropriate regulation of nSP size and surface properties may be crucial for the design of safer nSPs. Furthermore, accurate regulation of the ability of nSPs to induce cross-presentation may lead to new applications for nSPs, such as in cancer vaccines. We believe a detailed analysis of the mechanisms of nSP-mediated cross-presentation will be invaluable for both the design of safe nSPs and the development of new applications for them.

Acknowledgments

References

[1] J. Klein, Probing the interactions of proteins and nanoparticles, Proc. Natl. Acad. Sci. USA 104 (2007) 2029–2030.
[2] M. Auffan, J. Rose, J.Y. Bottero, G.V. Lowry, J.P. Jolivet, M.R. Wiesner, Towards a definition of inorganic nanoparticles from an environmental health and safety perspective, Nat. Nanotechnol. 4 (2009) 634–641.
[3] D.M. Bowman, G. van Calster, S. Friedrichs, Nanomaterials and regulation of cosmetics, Nat. Nanotechnol. 5 (2010) 92.
[4] R.K. Jain, T. Stylianopoulos, Delivering nanomedicine to solid tumors, Nat. Rev. Clin. Oncol. 7 (2010) 653–664.
[5] R. Peters, E. Kramer, A.G. Oomen, Z.E. Rivera, G. Oegema, P.C. Tromp, R. Fokkink, A. Rietveld, H.J. Marvin, S. Weigel, A.A. Peijnenburg, H. Bouwmeester, Presence of nano-sized silica during in vitro digestion of foods containing silica as a food additive, ACS Nano 6 (2012) 2441–2451.
[6] B. Trouiller, R. Reliene, A. Westbrook, P. Solaimani, R.H. Schiestl, Titanium dioxide nanoparticles induce DNA damage and genetic instability in vivo in mice, Cancer Res. 69 (2009) 8784–8789.
[7] K. Yamashita, Y. Yoshioka, K. Higashisaka, K. Mimura, Y. Morishita, M. Nozaki, T. Yoshida, T. Ogura, H. Nabeshi, K. Nagano, Y. Abe, H. Kamada, Y. Monobe, T. Imazawa, H. Aoshima, K. Shishido, Y. Kawai, T. Mayumi, S. Tsunoda, N. Itoh, T.

Yoshikawa, I. Yanagihara, S. Saito, Y. Tsutsumi, Silica and titanium dioxide nanoparticles cause pregnancy complications in mice, Nat. Nanotechnol. 6 (2011) 321–328.
[8] H. Nabeshi, T. Yoshikawa, K. Matsuyama, Y. Nakazato, A. Arimori, M. Isobe, S. Tochigi, S. Kondoh, T. Hirai, T. Akase, T. Yamashita, K. Yamashita, T. Yoshida, K. Nagano, Y. Abe, Y. Yoshioka, H. Kamada, T. Imazawa, N. Itoh, M. Kondoh, K. Yagi, T. Mayumi, S. Tsunoda, Y. Tsutsumi, Amorphous nanosilicas induce consumptive coagulopathy after systemic exposure, Nanotechnology 23 (2012) 045101.
[9] D. Napierska, L.C. Thomassen, D. Lison, J.A. Martens, P.H. Hoet, The nanosilica hazard: another variable entity, Part. Fibre Toxicol. 7 (2010) 39.
[10] H. Nabeshi, T. Yoshikawa, K. Matsuyama, Y. Nakazato, K. Matsuo, A. Arimori, M. Isobe, S. Tochigi, S. Kondoh, T. Hirai, T. Akase, T. Yamashita, K. Yamashita, T. Yoshida, K. Nagano, Y. Abe, Y. Yoshioka, H. Kamada, T. Imazawa, N. Itoh, S. Nakagawa, T. Mayumi, S. Tsunoda, Y. Tsutsumi, Systemic distribution nuclear entry and cytotoxicity of amorphous nanosilica following topical application, Biomaterials 32 (2011) 2713–2724.
[11] T. Hirai, T. Yoshikawa, H. Nabeshi, T. Yoshida, T. Akase, Y. Yoshioka, N. Itoh, Y. Tsutsumi, Dermal absorption of amorphous nanosilica particles after topical exposure for three days, Pharmazie 67 (2012) 742–743.
[12] R.M. Steinman, J. Banchereau, Taking dendritic cells into medicine, Nature 449 (2007) 419–426.
[13] K. Baker, S.W. Qiao, T.T. Kuo, V.G. Aveson, B. Platzer, J.T. Andersen, I. Sandlie, Z. Chen, C. de Haar, W.I. Lencer, E. Fiebiger, R.S. Blumberg, Neonatal Fc receptor for IgG (FcRn) regulates cross-presentation of IgG immune complexes by CD8-CD11b+ dendritic cells, Proc. Nat. Acad. Sci. USA 108 (2011) 9927–9932.
[14] T. Hirai, T. Yoshikawa, H. Nabeshi, T. Yoshida, S. Tochigi, M. Uji, K. Ichihashi, T. Akase, T. Yamashita, K. Yamashita, K. Nagano, Y. Abe, H. Kamada, S. Tsunoda, Y. Yoshioka, N. Itoh, Y. Tsutsumi, Size-dependent immune-modulating effect of amorphous nanosilica particles, Pharmazie 66 (2011) 727–728.
[15] T. Hirai, T. Yoshikawa, H. Nabeshi, T. Yoshida, S. Tochigi, K. Ichihashi, M. Uji, T. Akase, K. Nagano, Y. Abe, H. Kamada, N. Itoh, S. Tsunoda, Y. Yoshioka, Y. Tsutsumi, Amorphous silica nanoparticles size-dependently aggravate atopic dermatitis-like skin lesions following an intradermal injection, Part. Fibre Toxicol. 9 (2012) 3.
[16] C. Kurts, B.W. Robinson, P.A. Knolle, Cross-priming in health and disease, Nat. Rev. Immunol. 10 (2010) 403–414.
[17] F. Zhou, L. Huang, Delivery of protein antigen to the major histocompatibility complex class I-restricted antigen presentation pathway, J. Drug Target. 3 (1995) 91–109.
[18] C. Watts, Capture and processing of exogenous antigens for presentation on MHC molecules, Annu. Rev. Immunol. 15 (1997) 821–850.
[19] H. Nabeshi, T. Yoshikawa, A. Arimori, T. Yoshida, S. Tochigi, T. Hirai, T. Akase, K. Nagano, Y. Abe, H. Kamada, S. Tsunoda, N. Itoh, Y. Yoshioka, Y. Tsutsumi, Effect of surface properties of silica nanoparticles on their cytotoxicity and cellular distribution in murine macrophages, Nanoscale Res. Lett. 6 (2011) 93.
[20] Z. Shen, G. Reznikoff, G. Dranoff, K.L. Rock, Cloned dendritic cells can present exogenous antigens on both MHC class I and class II molecules, J. Immunol. 158 (1997) 2723–2730.
[21] J.D. Pfeifer, M.J. Wick, R.L. Roberts, K. Findlay, S.J. Normark, C.V. Harding, Phagocytic processing of bacterial antigens for class I MHC presentation to T cells, Nature 361 (1993) 359–362.
[22] S. Amigorena, A. Savina, Intracellular mechanisms of antigen cross presentation in dendritic cells, Curr. Opin. Immunol. 22 (2010) 109–117.
[23] O.P. Joffre, E. Segura, A. Savina, S. Amigorena, Cross-presentation by dendritic cells, Nat. Rev. Immunol. 12 (2012) 557–569.
[24] R.F. Hamilton Jr., S.A. Thakur, J.K. Mayfair, A. Holian, MARCO mediates silica uptake and toxicity in alveolar macrophages from C57BL/6 mice, J. Biol. Chem. 281 (2006) 34218–34226.
[25] G.A. Orr, W.B. Chrisler, K.J. Cassens, R. Tan, B.J. Tarasevich, L.M. Markillie, R.C. Zangar, B.D. Thrall, Cellular recognition and trafficking of amorphous silica nanoparticles by macrophage scavenger receptor A, Nanotoxicology 5 (2011) 296–311.
[26] T.S. Hauck, A.A. Ghazani, W.C. Chan, Assessing the effect of surface chemistry on gold nanorod uptake toxicity and gene expression in mammalian cells, Small 4 (2008) 153–159.
[27] T. Yu, D. Hubbard, A. Ray, H. Ghandehari, In vivo biodistribution and pharmacokinetics of silica nanoparticles as a function of geometry porosity and surface characteristics, J. Control. Release (2012).
[28] S. Febvay, D.M. Marini, A.M. Belcher, D.E. Clapham, Targeted cytosolic delivery of cell-impermeable compounds by nanoparticle-mediated light-triggered endosome disruption, Nano Lett. 10 (2010) 2211–2219.
[29] Z. Krpetic, P. Nativo, V. See, I.A. Prior, M. Brust, M. Volk, Inflicting controlled nonthermal damage to subcellular structures by laser-activated gold nanoparticles, Nano Lett. 10 (2010) 4549–4554.
[30] H. Nabeshi, T. Yoshikawa, K. Matsuyama, Y. Nakazato, S. Tochigi, S. Kondoh, T. Hirai, T. Akase, K. Nagano, Y. Abe, Y. Yoshioka, H. Kamada, N. Itoh, S. Tsunoda, Y. Tsutsumi, Amorphous nanosilica induce endocytosis-dependent ROS generation and DNA damage in human keratinocytes, Part. Fibre Toxicol. 8 (2011) 1.

○ **Nanoscale Research Letters**
a SpringerOpen Journal

Hemopexin as biomarkers for analyzing the biological responses associated with exposure to silica nanoparticles

Kazuma Higashisaka[1†], Yasuo Yoshioka[1*†], Kohei Yamashita[1], Yuki Morishita[1], Huiyan Pan[1], Toshinobu Ogura[1], Takashi Nagano[1], Akiyoshi Kunieda[1], Kazuya Nagano[2], Yasuhiro Abe[3], Haruhiko Kamada[2,4], Shin-ichi Tsunoda[2,4], Hiromi Nabeshi[5], Tomoaki Yoshikawa[1] and Yasuo Tsutsumi[1,2,4*]

Abstract

Practical uses of nanomaterials are rapidly spreading to a wide variety of fields. However, potential harmful effects of nanomaterials are raising concerns about their safety. Therefore, it is important that a risk assessment system is developed so that the safety of nanomaterials can be evaluated or predicted. Here, we attempted to identify novel biomarkers of nanomaterial-induced health effects by a comprehensive screen of plasma proteins using two-dimensional differential in gel electrophoresis (2D-DIGE) analysis. Initially, we used 2D-DIGE to analyze changes in the level of plasma proteins in mice after intravenous injection via tail veins of 0.8 mg/mouse silica nanoparticles with diameters of 70 nm (nSP70) or saline as controls. By quantitative image analysis, protein spots representing >2.0-fold alteration in expression were found and identified by mass spectrometry. Among these proteins, we focused on hemopexin as a potential biomarker. The levels of hemopexin in the plasma increased as the silica particle size decreased. In addition, the production of hemopexin depended on the characteristics of the nanomaterials. These results suggested that hemopexin could be an additional biomarker for analyzing the biological responses associated with exposure to silica nanoparticles. We believe that this study will contribute to the development of biomarkers to ensure the safety of silica nanoparticles.

Keywords: Silica nanoparticle, Plasma proteins, Hemolysis, Biomarker

Background

Nanomaterials with particle sizes below 100 nm display unique properties compared to conventional materials with a submicron size. Various types of nanomaterials have been designed and produced for consumer and industrial applications such as medicine, cosmetics, and food [1,2]. As the use of nanomaterials increases, there is a growing need to ensure their safety because their unique properties might be associated with undesirable biological interactions [3,4]. However, current knowledge of the potential risk of nanomaterials is considered insufficient. Therefore, to facilitate the development of nanomaterials as a safe and usable product, it is important to develop guidelines for evaluation of their safety and efficacy.

Silica nanoparticles have been widely used in many consumer products such as cosmetics, food, and medicine because of their useful properties, including straightforward synthesis, relatively low cost, easy separation, and easy surface modification [5,6]. However, recent studies have found that silica nanoparticles induce substantial lung inflammation and are cytotoxic to various cell types [7,8]. Furthermore, our group showed that silica nanoparticles penetrate the skin and produce systemic exposure after topical application [9]. These findings underscore the need to examine biological effects after systemic exposure to silica nanoparticles. Our group also demonstrated that intravenous injection of silica nanoparticles with a diameter of 70 nm into mice

* Correspondence: yasuo@phs.osaka-u.ac.jp; ytsutsumi@phs.osaka-u.ac.jp
†Equal contributors
[1]Laboratory of Toxicology and Safety Science, Graduate School of Pharmaceutical Sciences, Osaka University, 1-6 Yamadaoka, Suita, Osaka 565-0871, Japan
[2]Laboratory of Biopharmaceutical Research, National Institute of Biomedical Innovation, 7-6-8, Saito-Asagi, Ibaraki, Osaka 567-0085, Japan
Full list of author information is available at the end of the article